Synthesis and Experimental Procedures	S2
NMR (Nuclear Magnetic Resonance) Spectra	S11
MS (Mass Spectrometry)	S23
UV-visible Absorbance Spectra	S28
Photobleaching studies	S31
Photothermal studies	S33
Temperature Dependence UV-visible absorbance	S35
MDA-MB231 cell uptake, photo- and dark toxicity	S36
Octanol / water partition coefficient	S37
DLS (Dynamic Light Scattering)	S38
Photoacoustic studies	S41
SERRS studies and TEM	S42
Singlet Oxygen	S48
References	S50

Contributions

Synthesis and characterization of the tomamine phthalocyanines, cell studies: W. Rizvi, D. Bhupathiraju. Photoacoustic data and discussion: C. Farley, C. Andreou, M.F. Kircher. SERRS experiments and discussion: N. Barisha, M.F. Kircher. Singlet oxygen studies: G. Fuentes, R. Gao. Provision of SERRS and Photoacoustic instrumentation: M. F. Kircher. Project concept, supervision, manuscript writing/editing, interpreting data: C.M. Drain

Acknowledgements: Supported by the U.S. National Science Foundation CHE-1610755 to C.M.D. National Institutes of Health R01 EB017748 and CA222836 to M.F.K. We thank Mircea Cotlet at The Center for Functional Nanomaterials (CFN) for help with singlet oxygen studies; the CFN is a U.S. DOE Office of Science Facility at Brookhaven National Laboratory under Contract No. DE-SC0012704. We thank Alei A. Rizvi for help with the synthesis. *Other Support:* Center for Molecular Imaging & Nanotechnology (CMINT), Center for Experimental Therapeutics (ETC), Molecularly Targeted Intra-Operative Imaging Grant, and MSKCC Office of Technology TDF Grant to M.F.K; M.F.K. is a Damon Runyon-Rachleff Innovator supported (in part) by the Damon Runyon Cancer Research Foundation (DRR-29-14). Mr. William H. and Mrs. Alice Goodwin and the Commonwealth Foundation for Cancer Research.The Center for Functional Nanomaterials is a U.S. DOE Office of Science Facility at Brookhaven National Laboratory under Contract No. DE-SC0012704.

Detailed Synthesis

General. ^{1}H and ^{13}C solution NMR spectra were recorded using Bruker 500 MHz (spectrometer operating at 500 MHz for ^{1}H; 125 MHz, for ^{13}C), and ^{19}F solution NMR (376 MHz) spectra were recorded using Bruker 400 MHz. $CDCl_3$ was used as solvent and TMS as internal reference; the chemical shifts are expressed in (ppm) and the coupling constants (*J*) in Hertz (Hz). High Resolution Electrospray Ionization Mass Spectra (HRESIMS) were obtained using an Agilent 6520 Q-TOF instrument. The UV-vis absorbance spectra in various solvents were recorded using PerkinElmer Lambda 35 UV/VIS spectrometer. PerkinElmer Peltier Temperature Programmer PTP 1 was used to obtain temperature dependent UV-vis absorbance spectra. Steady-state fluorescence (emission) spectra were measured with Fluorolog τ3, Jobin-SPEX Instrument S.A., Inc. An inVision 256-TF Multispectra Optoacoustic Tomagraphy (MSOT) imaging system (iThera Medical) was used for photoacoustic studies. Dynamic light scattering (DLS) studies to find particle size were performed on Malvern Zetasizer nano series instrument. Reagent grade chemicals and solvents were purchased from Sigma-Aldrich Inc., Fisher Scientific Inc. or Air Chemicals. Reactions were monitored by TLC with Analtech Uniplate silica gel G/UV 254 precoated plates (0.2 mm).

Synthesis of ZnPc(tomamine)$_1$. Zinc 1,2,3,4,8,9,10,11,15,16,17,18,22,23,24,25-hexadecafluoro-29H,31H-phthalocyanine ($ZnF_{16}Pc$) (100 mg, 0.115 mmol) dissolved in dimethylformamide (DMF) (10 mL) was reacted with 1.2 equivalents of N1-(3-((8-methylnonyl)oxy)propyl)propane-1,3-diamine (37.7 mg, 0.139 mmol) at 110 °C, under a N_2 atmosphere for 12 hours. The reaction mixture was cooled and 20 mL of ethyl acetate (EtOAc) was added and washed with brine (3x). The organic layer was dried using sodium sulfate to remove trace amount of water. EtOAc was removed through a rotator evaporator and the crude product was purified by flash chromatography (silica gel) using 1 % methanol in CH_2Cl_2 as eluent to afford 32 % pure ZnPc(tomamine)$_1$ (40 mg, 0.0368 mmol) as a dark blue solid. ^{1}H NMR (500 MHz, $CDCl_3$) δ 5.03 (bs, 1H), 3.97 (t, *J*=2.25 Hz, 2H), 3.74 (t, *J*=1.60 Hz, 2H), 3.38 (t, *J*=7.70 Hz, 4H), 3.03 (t, *J*=6.90 Hz, 2H), 1.41-1.67 (m, 9H), 0.99-1.36 (m, 8H), 0.88 (d, *J*=5.05 Hz, 6H); ^{13}C NMR (125 MHz, $CDCl_3$) δ; 148.55, 147.64, 141.49, 139.15, 136.07, 131.15, 130.59, 126.50, 123.03, 121.85, 120.27, 117.55, 114.15, 113.07, 71.26, 69.99, 65.78, 53.46, 52.38, 51.07, 40.12, 32.22, 31.60, 30.32, 28.44, 27.68, 24.52, 24.16, 22.62; ^{19}F NMR (376 MHz, $CDCl_3$): δ -158.96 (s, 6F, βF), -170.10 (d, 8F, αF). HRMS (ESI) *m/z* calcd for $C_{48}H_{34}F_{14}N_{10}OZn$ ($[M+H]^+$), 1097.2058, found 1097.2058.

Synthesis of ZnPc(tomamine)$_2$. Zinc 1,2,3,4,8,9,10,11,15,16,17,18,22,23,24,25-hexadecafluoro-29H,31H-phthalocyanine ($ZnF_{16}Pc$) (100 mg, 0.115 mmol) dissolved in dimethylformamide (DMF) (10 mL) was reacted with 2.2 equivalents of N1-(3-((8-methylnonyl)oxy)propyl)propane-1,3-diamine (69.1 mg, 0.255 mmol) at 120 °C, under a N_2 atmosphere for 16 hours. The reaction mixture was cooled and 20 mL of EtOAc was added and washed with brine (3x). The organic layer was dried using sodium sulfate to remove trace amount of water. EtOAc was removed through a rotator evaporator and the crude product was purified by flash chromatography (silica gel) using 1.5 % methanol in CH_2Cl_2 as eluent to afford 28 % pure ZnPc(tomamine)$_2$ (43 mg, 0.0322 mmol) as a darker blue solid. ^{1}H NMR (500 MHz, $CDCl_3$) δ 5.02 (bs, 1H), 3.98 (t, *J*=2.25 Hz, 2H), 3.81 (t, *J*=1.60 Hz, 2H), 3.08 (t, *J*=6.90 Hz, 4H), 2.99 (t, *J*=5.95 Hz, 2H), 1.16-1.69 (m, 9H), 1.01-1.07 (m, 8H), 0.77-1.00 (m, 6H); ^{13}C NMR (125 MHz, $CDCl_3$) δ; 148.55, 147.59, 141.45, 140.15, 136.07, 131.13, 130.59, 126.24, 123.09, 121.90, 120.22, 117.58, 114.15, 113.14, 71.24, 69.90, 65.78, 53.47, 52.34, 51.65, 40.93, 39.72, 32.27, 31.63, 30.35, 28.47, 27.64, 25.52, 24.16, 22.62; ^{19}F NMR (376 MHz, $CDCl_3$): δ -159.70-160.92 (m, 4F, βF), -169.13-169.93 (bd, 8F, αF).. HRMS (ESI) *m/z* calcd for $C_{64}H_{68}F_{12}N_{12}O_2Zn$ ($[M+H]^+$), 1329.4761, found 1329.4748.

Synthesis of ZnPc(tomamine)$_3$. Zinc 1,2,3,4,8,9,10,11,15,16,17,18,22,23,24,25-hexadecafluoro-29H,31H-phthalocyanine ($ZnF_{16}Pc$) (100 mg, 0.115 mmol) dissolved in dimethylformamide (DMF) (10 mL) was reacted with 3.2 equivalents of N1-(3-((8-methylnonyl)oxy)propyl)propane-1,3-diamine (100.5 mg, 0.371 mmol) in the presence of potassium carbonate (52 mg, 0.376 mmol) at 120 °C, under a N_2 atmosphere for 24 hours. The reaction mixture was cooled and 20 mL of EtOAc was added and washed with brine (3x). The organic layer was dried using sodium sulfate to remove trace amount of water. EtOAc was removed through a rotator evaporator and the crude product was purified by flash chromatography

(silica gel) using 2 % methanol in CH_2Cl_2 as eluent to afford 35 % pure ZnPc(tomamine)$_3$ (63 mg, 0.0403 mmol) as a darker blue solid. ^{1}H NMR (500 MHz, $CDCl_3$) δ 5.01 (bs, 1H), 4.02 (t, *J*=1.30 Hz, 2H), 3.94 (t, *J*=8.0 Hz, 2H), 3.11 (t, *J*=6.90 Hz, 4H), 3.03 (t, *J*=5.70 Hz, 2H), 1.45-1.62 (m, 9H), 0.91-1.12 (m, 8H), 0.63-0.68 (m, 6H); ^{13}C NMR (125 MHz, $CDCl_3$) δ; 149.55, 148.59, 141.34, 140.14, 136.02, 131.13, 130.58, 126.25, 123.01, 121.89, 120.21, 117.56, 114.18, 113.13, 71.24, 69.90, 65.78, 53.47, 52.34, 54.05, 41.12, 39.72, 32.26, 31.63, 30.34, 20.48, 27.64, 24.52, 23.16, 22.62; ^{19}F NMR (376 MHz, $CDCl_3$): δ -159.23 (s, 2F, βF), -169.13 (s, 8F, αF). HRMS (ESI) *m/z* calcd for $C_{80}H_{102}F_{10}N_{14}O_3Zn$ ($[M+H]^+$), 1563.7472, found 1563.7464.

Synthesis of ZnPc(tomamine)$_4$. Zinc 1,2,3,4,8,9,10,11,15,16,17,18,22,23,24,25-hexadecafluoro-29H,31H-phthalocyanine ($ZnF_{16}Pc$) (100 mg, 0.115 mmol) dissolved in dimethylformamide (DMF) (10 mL) was reacted with 5.2 equivalents of N1-(3-((8-methylnonyl)oxy)propyl)propane-1,3-diamine (163.3 mg, 0.603 mmol) in the presence of potassium carbonate (84 mg, 0.607 mmol) at 135 °C, under a N_2 atmosphere for 48 hours. The reaction mixture was cooled and 20 mL of EtOAc was added and washed with brine (3x). The organic layer was dried using sodium sulfate to remove trace amount of water. EtOAc was removed through a rotator evaporator and the crude product was purified by flash chromatography (silica gel) using 5 % methanol in CH_2Cl_2 as eluent to afford 18 % pure ZnPc(tomamine)$_4$ (37 mg, 0.0207 mmol) as a dark blue to black solid. ^{1}H NMR (500 MHz, $CDCl_3$) δ 5.01 (bs, 1H), 4.28 (t, *J*=2.95 Hz, 2H), 4.21 (t, *J*=1.55 Hz, 2H), 3.27 (t, *J*=3.20 Hz, 4H), 3.20 (t, *J*=5.5 Hz, 2H), 1.54-1.67 (m, 9H), 1.00-1.37 (m, 8H), 0.77-0.99 (m, 6H); ^{13}C NMR (125 MHz, $CDCl_3$) δ; 148.10, 147.13, 141.49, 139.15, 136.04, 132.14, 130.59, 126.50, 122.99, 121.83, 120.27, 117.55, 113.85, 113.07, 70.26, 69.48, 65.39, 52.55, 51.38, 50.60, 39.51, 31.53, 30.75, 29.78, 27.44, 26.66, 24.52, 23.16, 21.60; ^{19}F NMR (376 MHz, $CDCl_3$): δ -170.05 (s, βF). HRMS (ESI) *m/z* calcd for $C_{97}H_{138}F_8N_{16}O_4Zn$ ($[M+H]^+$), 1796.0184, found 1795.9958; calcd for $C_{97}H_{138}F_8N_{16}O_4Zn$ ($[M+Na]^+$), 1820.9997, found 1820.9997.

Characterization

NMR Spectra

The ^{1}H NMR spectra of ZnPc(tomamine)$_1$, ZnPc(tomamine)$_2$, ZnPc(tomamine)$_3$, and ZnPc(tomamine)$_4$ do not show a significant difference as there are no H present on the macrocycle. Only the substituted alkyl chains have H which are same in all four compounds. There is a little shift of peaks in all four compounds, but the integration and splitting are very similar. The ^{1}H NMR spectrum for ZnPc(tomamine)$_1$ is well resolved compared to ZnPc(tomamine)$_2$, ZnPc(tomamine)$_3$, and ZnPc(tomamine)$_4$ because of presence of isomers for the latter compounds. The ^{13}C NMR for all four compounds show all of aromatic carbons of the macrocycle as well as the aliphatic carbons of the substituted groups. ^{19}F NMR is the most informative in characterizing these compounds. The ^{19}F NMR spectra confirm the substitution of the β-fluorine atoms. The integration values for ZnPc(tomamine)$_1$, ZnPc(tomamine)$_2$, ZnPc(tomamine)$_3$ show loss of two, four and six β-fluorine atoms respectively. However, for compound ZnPc(tomamine)$_4$, the β-fluorine peak completely disappears indicating a complete substitution.

UV-visible spectroscopy

PerkinElmer Lambda UV/VIS Spectrometer was used to record the UV-visible spectra of dilute solutions, typically ~2 μM, of ZnPc(tomamine)$_1$, ZnPc(tomamine)$_2$, ZnPc(tomamine)$_3$, and ZnPc(tomamine)$_4$ in dimethylsulfoxide (DMSO), tetrahydrofuran (THF), CH_2Cl_2, acetone, and methanol solvents. The spectra were recorded from 400 to 900 nm using 1 cm quartz cuvettes. There was a large shift observed for all four compounds compared to the parent $ZnF_{16}Pc$ molecule. High solvent dependency was observed for all four compounds with peak shifting blue or red depending on the solvent polarity and dielectric constant (see table S1). Using PerkinElmer Peltier Temperature Programmer PTP 1, the UV-visible spectra were taken in THF at various temperatures 0, 25 and 60 °C. For the ZnPc(tomamine)$_1$ and ZnPc(tomamine)$_4$, no significant temperature dependence in λ_{max} was observed, the FWHM of 754 nm for ZnPc(tomamine)$_1$ 804 nm for ZnPc(tomamine)$_4$ do not change either. For example see figures S32-S33.

Emission spectroscopy, fluorescence quantum yield

Steady-state fluorescence (emission) spectra were recorded in DMSO, acetone and phosphate buffer saline (PBS) solvent in air and under nitrogen atmosphere by purging N_2 gas through these solutions for ca. 10 minutes. The concentrations of each compound in these solutions were typically adjusted to have absorption of less than 0.1 at the excitation wavelength. ZnPc(tomamine)$_1$, ZnPc(tomamine)$_2$, ZnPc(tomamine)$_3$, and ZnPc(tomamine)$_4$ were excited at 675 nm, 725 nm, 725 nm and 750 nm respectively. Both, the excitation and emission monochromators had a band pass of 5 nm. The corrected emission (for instrument response) and absorption (UV-visible) spectra were used to calculate the quantum yield. The quantum yields were calculated relative to tetraphenylporphyrinato zinc(II) in toluene, which has a fluorescence quantum yield of 0.033.[2] All experiments were carried out on the same day, using identical concentrations and similar experimental conditions to minimize any experimental errors. All compounds showed quantum yields of less than 0.01. This is an indication that the excited state energy is being released by a method other than fluorescence emission.

Dynamic Light Scattering (DLS) for particle size measurement

Solutions of all four compounds were found to form aggregates in acetone and PBS. A Malvern Zetasizer nano series DLS instrument was used in batch mode at 25 °C to determine particle size. These solutions were sonicated in Fisher SF15 sonicator to break the large aggregates into the small ones. To measure the size, ~50 µM solutions were prepared in 2% DMSO in PBS, the solution was sonicated for ca. 30 minutes and left to rest for another 30 min, filtered using 0.45 µm syringe filter and then the size was measured. At ~50 µM concentrations, particles with sizes of 53±6 nm, 69±9 nm, 98±7 nm, and 122±10 nm were observed for ZnPc(tomamine)$_1$, ZnPc(tomamine)$_2$, ZnPc(tomamine)$_3$, and ZnPc(tomamine)$_4$ respectively in acetone and 89±8 nm, 133±7 nm, 193±10 nm and 223±9 nm in 2% DMSO in PBS.

Aggregates

The photophysics of porphyroinoid aggregates is well established.[3] The photo-induced disassembly of porphyrinoid aggregates in the presence of the complex milieu of the cell (lipids, proteins, etc.) is well-established in the context of PDT;[4] however, we did not pursue this in terms of the cell studies of the tri- and tetra- tomah derivatives. Since charge transfer complexes are not formed upon photo illumination of this system, this mode of aggregation is not relevant.

Photobleaching and compound stability

Photostabilities of ZnPc(tomamine)$_1$, ZnPc(tomamine)$_2$, ZnPc(tomamine)$_3$, and ZnPc(tomamine)$_4$ were determined using the UV-visible absorbance of the compounds. Solutions of compounds were made in acetone to have UV-vis absorbance ca. 0.05 in the lowest energy Q band (ca. 1 µM) in 1 cm glass cuvettes which were exposed to direct white light at 0.41 mW/cm2 using a General Electric Helical 13W, 120V AC, 60 HZ, 190mA, (FLE13HT 2/2/XL.SW) fluorescent bulb in air with the cuvette capped. There is no evidence of decomposition in the dark. UV-visible measurements were taken after two, four and eight hours to assess the stabilities of the compounds. All experiments were done side by side on the same day to minimize any experimental errors. All compounds were intact >50% after 4 h of light exposure. The redox chemistry of the amine moieties of the tomamine component may be involved in the photobleaching of the ZnPc(tomamine)$_n$ compounds.

Cell culture, uptake and toxicity studies

All tissue culture medium and reagents were purchased. Dulbecco's Modified Eagle Medium (DMEM) from Sigma Aldrich and FBS and antibiotic (Penicillin Streptomycin) from Invitrogen (Carlsbad, CA). MDA-MB-231 cells were purchased from ATCC and cultured in DMEM in 10% FBS and 1% antibiotic. The cells were split once every two days to maintain a sub-confluent stock.

MDA-MB-231, human breast cancer cells were maintained in DMEM, 10% FBS, 1% antimycotic at 37 °C and in 5% CO_2 atmosphere were plated in cell culture dishes with coverslips for 24 hours. Cells were then

incubated with ZnPc(tomamine)$_1$, ZnPc(tomamine)$_2$, ZnPc(tomamine)$_3$, and ZnPc(tomamine)$_4$ dissolved in DMSO to a final concentration of 50 nM such that there was never more than 0.5% DMSO in the solution. After 24 h incubation, cells were washed with PBS 5-6 times to remove the unbound compound and then fixed with 4% paraformaldehyde solution for 15 min at room temperature. The cells were then washed with PBS 3 times again. The number of cells were counted under an inverted microscope. Since the compounds are not fluorescent, simple fluorescence microscopy could not be used to assess dye uptake. The cultures were treated with Triton X-100 bought from Sigma-Aldrich to lyse the cells. The resulting solutions were dissolved in acetone and UV-visible absorption spectra of each well on the plate was taken to find the amount of compound present per cell.

Dark toxicity

MB-MDA-231 cells (20,000) were seeded in a 96 well plate and incubated at 37 ^{o}C and in CO_2 atmosphere for 48 h until 90% confluence was observed. ZnPc(tomamine)$_1$, ZnPc(tomamine)$_2$, ZnPc(tomamine)$_3$, and ZnPc(tomamine)$_4$ were dissolved in DMSO and then diluted with DMEM into final working concentrations (6.25, 12.5, 25, 50, 100 μM). Compounds with different concentrations were added to the 90% confluent cells and incubated for 24 h. Then the medium containing dye was removed and washed once with PBS (pH ~ 7.4). 0.4% Trypan blue (Life Technologies™) was added to cells. The mixture was incubated at room temperature for 10 min, and trypan blue uptake was determined by counting on a hemacytometer. The IC_{50} values were calculated from dose-response curves, which were obtained using GraphPad Prism software.

Phototoxicity

MDA-MB-231 cells were plated as described above. Then working concentrations (6.25, 12.5, 25, 50, 100 μM) of ZnPc(tomamine)$_1$, ZnPc(tomamine)$_2$, ZnPc(tomamine)$_3$, and ZnPc(tomamine)$_4$ were added and incubated for 24 h. Then the medium was replaced with the fresh medium. The cells were then exposed to a white 13 W fluorescent light for 20 min (0.92 mW cm^{-2} or 11.04 kJ m^{-2}, which is in the typical range for PDT studies using while light).[5] Then the medium containing the dye was removed. 0.4% Trypan blue (Life Technologies™) was added to cells. The mixture was incubated at room temperature for 10 min, and trypan blue uptake (dead cells) was determined by counting on a hemacytometer. The IC_{50} values were calculated from dose-response curves, which were obtained using GraphPad Prism software. In this case the fluorescent lamp has the spectra typical of these bulbs (General Electric Helical 13W, 120V AC, 60 HZ, 190mA, (FLE13HT 2/2/XL.SW) fluorescent bulb), and was chosen because of the minimal intensity in the UV and the near IR and IR (see figure S51 taken from https://www.comsol.com/ and figure S52 taken from https://publiclab.org).

Photothermal studies

ZnPc(tomamine)$_1$, ZnPc(tomamine)$_2$, ZnPc(tomamine)$_3$, and ZnPc(tomamine)$_4$ were dissolved in DMSO and then diluted with DMEM into final working concentrations (20, 40, 60, 80, 100 μM). The final solutions were made sure not to have more than 5% DMSO. The 1.5 mL solutions in closed 2 mL borosilicate vials were then exposed to a white 13 W fluorescent lamp with intensity of 0.92 mw/cm^2. Temperature was measured every 4 min with a digital thermometer. After 20 min, an increase of 12±2, 15±2, 15±2 and 17±2 ^{o}C was observed for ZnPc(tomamine)$_1$, ZnPc(tomamine)$_2$, ZnPc(tomamine)$_3$, and ZnPc(tomamine)$_4$ respectively. “White light” typically refers to the entire visible spectrum of the lamp used. This power is similar to that used in the PDT studies.

Octanol/PBS partition studies

Octanol-PBS partition coefficient values were determined for ZnPc(tomamine)$_1$, ZnPc(tomamine)$_2$, ZnPc(tomamine)$_3$, and ZnPc(tomamine)$_4$ using the classic shake flask method.[6]

Photoacoustic studies

Sample Preparation. Phthalocyanines [ZnPc(tomamine)$_1$, ZnPc(tomamine)$_2$, ZnPc(tomamine)$_3$ and ZnPc(tomamine)$_4$] and a standard indocyanine green (ICG) dye were suspended in DMSO and 10 μM aqueous solutions made (<1% DMSO cosolvent). A 1.5% agarose tissue phantom was also made with 1.2% v/v of a commercial 20% intralipid emulsion added to mimic scattering and absorption.[7] The fresh

dye solutions were loaded into plastic pouches and suspended in this tissue phantom at 50 °C in a 20 mL plastic syringe. The phantom was then allowed to cool to room temperature and set overnight before being removed from the syringe. There was no evidence of aggregation of the dyes in the amphipathic agarose phantom media. Each phantom contained 3 samples in separate pouches: one ICG standard and two different concentrations of the ZnPc(tomamine) dye. The ICG and high concentration ZnPc(tomamine) samples were prepared at equal concentrations.

Multispectral Optoacoustic Tomography (MSOT) Imaging. MSOT was performed on an inVision 256-TF instrument (iThera Medical), which has been described previously.[8] The cylindrical molded tissue phantom with the embedded dye-pouches was loaded into the instrument and submerged in a water bath kept at 34 ^{o}C. A wavelength-tunable light source is split and distributed about the sample to provide cylindrically symmetrical illumination of each cross-section. The detector has a similar cylindrical configuration, wrapping 270° about the sample axis. The sample is z-translated through this source / detector ring in 1.0 mm steps to collect tomographic cross-sections. For each pixel within a cross-section (*i.e.* each voxel), the instrument scans excitation wavelengths from 690 to 900 nm in 10 nm increments, collecting and averaging 5 photoacoustic intensity measurements at each wavelength. Three dimensional tomograms were constructed from these cross-sections, and some of the images are shown in Figure S39.

Photoacoustic Spectra. Average photoacoustic (PA) spectra, *i.e.* plots of PA intensity *vs*. excitation wavelength, were reconstructed from the tomographic information for each dye. Representative cross-sections were chosen for each dye-pouch, and the spectra of several pixels within each cross section were averaged together. These averaged PA spectra are shown in the manuscript. In all the figures, the green color indicates the indocyanine green (ICG) standard used in PA[9] and the other color (red, blue, orange and purple) represents the corresponding tomamine-ZnPc conjugate in the same phantom. It should be noted that the spectra of the individual dyes are very broad and overlap significantly, reducing the effectiveness of this deconvolution procedure. This manifests as the apparent mixing of 2 colors in a single pouch in some of the tomograms, even though the dyes were not physically mixed in any of these experiments.

Results. In the tomograms acquired, the detected PA intensity cannot discriminate between the various dyes present in the phantom. Therefore, a direct classical least-squares deconvolution technique was applied using the individual dye spectra to obtain the 2-color images seen in Figure 38A-D.

SERRS Studies

Raman spectroscopy takes advantage of inelastic scattering between vibrational modes to yield highly specific 'finger-print' spectra that can identify a compound. Unlike fluorescence, spectral peaks of compounds are narrower, and the intensity does not photo bleach over time. This gives Raman spectroscopy the ability to deconvolve signals in complex mixtures and the advantage of monitoring specific entities over a period of time without signal decay.[10] However, since the intrinsic Raman signal of molecules is weak, coupling molecules of interested with the electric field at the surface of plasmonic materials significantly enhances the signal. Surface enhanced Raman (SERS) can use plasmonic nanoparticles with any molecule of interest that has affinity to either gold or silver.[11] Recently SERS is used in variety of applications including biomedical imaging, trace detection of pesticides in food, explosive substances in airports, and monitoring catalysis over time.[12] We incorporated the ZnPc(tomamine)$_n$ molecules into a previously reported gold nanostructure[13] to measure their Raman capabilities for applications in biomedical imaging and sensor design.

Gold nanostars were synthesized by rapid reduction of gold chloride trihydrate in the presence of ascorbic acid according to previously reported methods. This yields about 5 mL of nanostars that are typically 1 nM in concentration. After dialysis to remove all reagents, these are stable in solution for months without stabilizing agents.[13] Nanostars were chosen as they have an absorption maximum in the red and near IR portion of the visible spectrum[14] and this correlates well with both the absorption of our dyes and the irradiation wavelength of the laser used, which results in better

over-lap of the contributing factors to enhancement of the Raman signal, surface enhanced resonance Raman spectra (SERRS).[15]

The platform is based on an earlier design[13] based on a surfactant-free shape control of gold nanoparticles enabled by unified theoretical framework of nanocrystal synthesis (Figure S40). The SERRS data for the control IR 780, the four tomamine compounds, and precursor and TEM images of the nanoplatform for each dye are in Figures S41-S46. A Renishaw (Gloucestershire, UK) *inVia* Raman microscope was used to collect the data.

Briefly, gold nanostars were synthesized by rapid (30 seconds) reduction of gold chloride trihydrate (20 mM solution; 8 mL) in the presence of ascorbic acid (60 mM solution; 800 mL). The solution turns from transparent to a deep blue color upon addition of the gold salt.

The dyes are incorporated by a fast adsorption of the dyes on to the surface of the particles and simultaneous silication to passivate the dye-covered particles.[13, 16] Adsorption is favored due to the affinity of the many nitrogen atoms in phthalocyanine molecules to gold. Briefly, a mixture of 0.5 mL as-produced stars and 80 µL 28%-ammonium hydroxide in 1.25 mL ethanol was added to a vortexed mixture of 200 µL silica precursor, tetraethyl-orthosilcate (TEOS), 80 µL distilled water, and 0.125 µmol dye (dissolved in 5-10 µL DMF) in 4 mL of isopropanol. Reactions were shaken at 300 rpm for 15 minutes, and then quenched by addition of more ethanol. Particles were washed three times with ethanol and re-dispersed in distilled water.

Ten microliters of the re-dispersed star solutions were put into a 384 flat bottom well plate. The area of the wells was scanned at a 200 µm step-size in the x-direction and a 14.2 µm step-size in the y-direction. To obtain Raman spectra, an inVia Renishaw Raman spectroscope was used with a 785 nm diode laser at 160 mW laser power, 5x objective, in StreamLine high-speed acquisition mode. With StreamLine imaging, multiple spectra are acquired under a continuous one second laser irradiation, with each point irradiated for about 0.1 seconds. Spectra are background corrected to remove fluorescence signal.

Transmission Electron images were taken to reflect the morphology of the particles. Samples were deposited on a 300 mesh carbon film copper grid and images were taken on a JEM-2100 200 keV high resolution transmission electron microscope with system-optimized exposure times.

DFT calculated Raman B3LYP 6-31G+ (d.p.) basis set was used.

Discussion of substitution chemistry and electronic spectra

Primary alkoxide nucleophiles were thought to react first at the α position (the synthesis uses 1.6 M n-BuLi and temperatures of 110-130 ^{o}C) but there was no NMR data to support this conclusion.[17] Significant computation efforts have been devoted to understanding the electronic spectra of PC, and for the free base Pc the α carbons contribute more to the HOMO than the β carbons, so electron donating groups destabilize the HOMO.[18] For electron donating groups, intramolecular charge transfer bands arising from the donor atom lone pair to the macrocycle π* orbital can significantly contribute to the observed spectral shifts. However, recent studies conclude that larger substitutents such as sugars preferentially react at the β position.[19] The systematic study of the substitution 1 to 16 of the F on $ZnPcF_{16}$ by alkane thiols, coupled with TDDFT calculations, concludes that kinetic products dominate and the β position react first at room temperature.[20] There is a small ca. 6 nm red shift in the Q bands for each of the first eight substitutions. After the initial eight substitutions, distortion of the Pc induced by α substitution is indicated by large Stokes shifts, a dramatic decrease in the fluorescence quantum yield and rate constant k_f, and a jump in the FWHM of the lowest energy Q band.[20]

^{19}F NMR data is consistent with β substitutions as previously reported[19-20] where the β F appears downfield compared to α F, and as the number of substitutions increases from 1-4 there is a disappearance of β F. HRMS, H-NMR and C-NMR shows that the two amine groups on the tomah forms a seven membered ring where the two β F's are replaced by one tomah moiety. There are several reports that the β position will be substituted first under mild conditions, then the alpha substitutions will be possible under forcing conditions such as high temperature and strong bases such as (NaH and Na).[20] The NMR shows that we indeed have only the β substitutions. The difference in α versus β reactivity also may be attributed to the mechanism of nucleophilic aromatic substitution reactions on the macrocycle.

The H-NMR clearly indicates the formation of the seven membered ring. A small red shift of about 10 nm in the Q bands is expected from substitution of the β F by the tomah amine on one isoindole,[18, 20] but a much larger shift is observed, from 672 nm to 745 nm. We agree that the large red shift, the quenched fluorescence, close to no singlet oxygen yield, and strong solvatochromism can be explained by an intramolecular charge transfer (ICT) band,[18] but these can also be explained by distortion of the macrocycle wherein there is a significant dipole.[21] Though we cannot completely rule out ICT, the strong photo-thermal conversion of the absorbed light and minimal photobleaching in air argue against significant ICT. Also, ICT is postulated for electron donors on the α position, and here the attachment to the β position.

The displayed solvatochromism is not necessarily due to solvent polarity alone, but is likely a mixture of polarity, polarizability, coordinating ability to the Zn(II) and hydrogen bonding ability. Different solvents will have different interactions with the central metal and the nitrogens and oxygens in the tomah substituents, and some of these interactions may depend on the particular conformation or overall flexibility of the Pc. For example, the peak shift shown in Table 1 between acetone and DMSO is significant (>25 nm), but these solvents have similar polarities so it would be inappropriate to assume that shift is entirely due to this factor alone. Further, we have shown previously that nitroporphyrins with a significant charge transfer character may not display a significant absorbance peak shift even between DMSO and toluene.[22] While the situation may be different for these phthalocyanines, there is no reason to assume *a priori* that charge transfer is a necessary condition, especially given the nature of these substituents.

We note that short triplet state lifetimes and/or low triplet state energy are possible explanations for the low singlet oxygen quantum yields. But, it would be unusual for this Pc triplet to have such a low energy or be so short lived as to have a completely negligible singlet oxygen yield. Phthalocyanines commonly have singlet oxygen yields above 50%, and even nitroPcs have a ca. 11% singlet oxygen yield. Charge transfer states would therefore seem less likely to explain the complete quenching of the triplet state.

In terms of the energetics needed to distort the Pc, the Zn(II) does not fit perfectly into the Pc core and can contribute to lowering the barrier to distortion.[23]

Discussion of SERRS spectra

Table S1. SERRS peaks

Dye	SERRS Wavenumber (cm^{-1})	Intensity cps
ZnF16Pc	733, 750, 1526	84.1, 115.2, 84.2
Mono-Tomah	726, 750, 1518	39.7, 119.7, 36.7
Di-Tomah	730, 751, 1518	271.6, 470.5, 103.5
Tri-Tomah	730, 751, 1517	310.2, 615.8, 119
Tetra-Tomah	730, 751, 1516	1001.2, 1689.9, 264.2

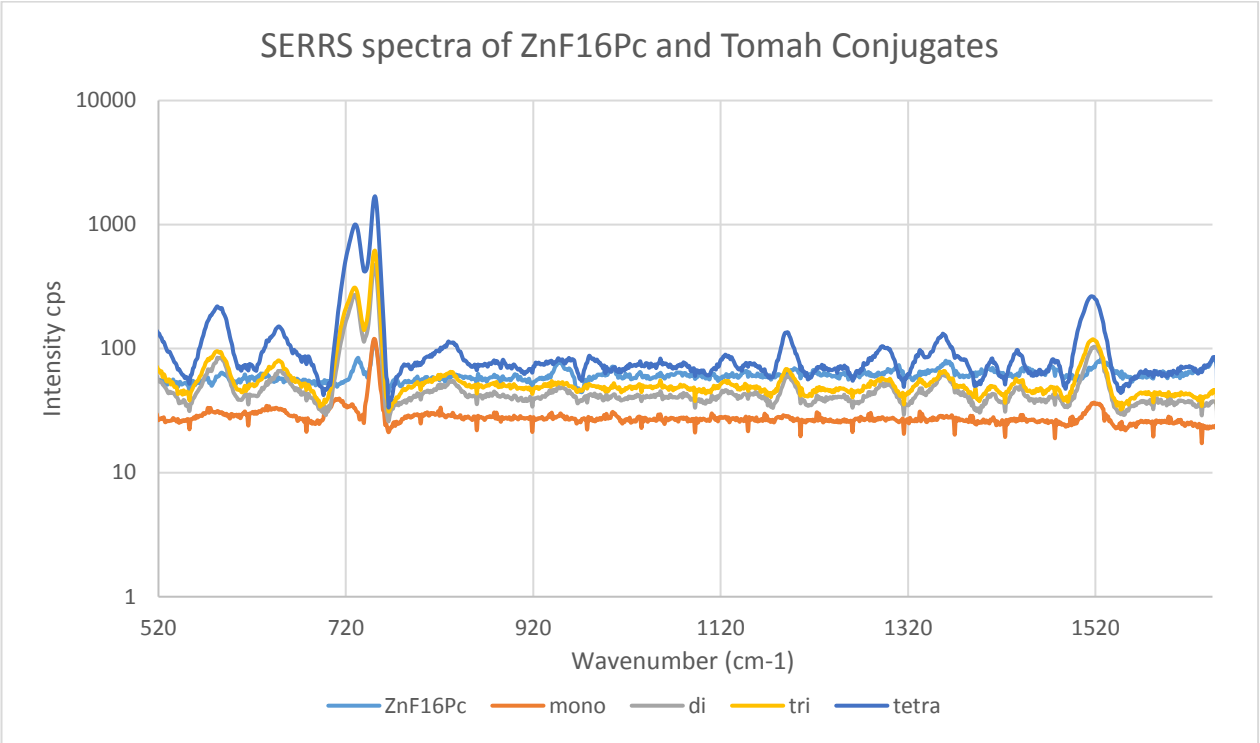

Base on assignments of the $ZnPc(SO_3)_4$, for the $ZnPcF_{16}$ the peak at 750 cm^{-1} is likely the antisymmetric deformation of the macrocycle, and that at 1526 cm^{-1} is likely the isoindole stretching.[24] These shift upon conjugation of tomamine; however, the spectral shifts between higher substitutions (di to tetra) are not significantly different. The peak at 733 cm^{-1} is likely the C-F bending, assignments based on 1,2,4,5-tetra-fluorobenzene[25] in analogy to the tetrafluoro isoindoles in the parent $ZnPcF_{16}$. The fluorescence quantum yield of IGC is 2-6%, so most of its energy is dissipated by internal conversion.[26]

TABLE S2. Fundamental vibration frequencies for 1,2,4,5-tetrafluorobenzene (liquid).[2]

	a_g	B_{1g}	b_{2g}	b_{ag}	a_u	b_{1u}	b_{2u}	b_{3u}
C- H stretching	3097					3088		
C-F stretching	1335		1196			1222		1277
C-C stretching	1374		1643			1439		1534
C-C breathing	748					963		853
C-F bending	832	417	635	669	(~600)	700	461	755
C-H bending			1130	871			869	1164
C-C-C bending	487		202	295	(140)		(240)	

Highlighted in yellow are numbers that correspond to the major peaks $ZnPcF_{16}$ spectra in the measured spectrum (520-1650cm^{-1}). Given the low signal to noise and possible overlapping, some peaks are not observed.

Quantum yield of singlet oxygen production

The comparative method was used to determine singlet oxygen quantum yields (Φ_Δ) of ZnPc(tomamine)$_1$, ZnPc(tomamine)$_2$, ZnPc(tomamine)$_3$, and ZnPc(tomamine)$_4$ in deuterium acetone (d-acetone). Rose bengal with known Φ_Δ = 0.70 in acetone is used as a standard reference (Figure S47).[27] Samples of ZnPc(tomamine)$_1$, ZnPc(tomamine)$_2$, ZnPc(tomamine)$_3$, and ZnPc(tomamine)$_4$ and rose bengal were dissolved in d-acetone. The absorbance of all samples and rose bengal reference was adjusted fitting into the range of 0.05-0.6 at 532 nm. The slopes derived from the plots of singlet oxygen intensity at 1270 nm vs absorbance at 532 nm were used for quantum yield calculations according to the following equation.[28] A Q-switched Nd:YAG laser with a pulse duration of 3-4 ns and a maximum energy of 30 mJ at 532 nm (Polaris II-20, New Wave Research Merchantek Products) and a repetition rate of 20 Hz in combination with a FT 200 Fluorimeter (Picoquant) equipped with an InGaAs Hamamatsu micro channel photomultiplier were employed for time-resolved $^1O_2$ luminescence measurements. The generation of singlet oxygen from these compounds was inefficient with Φ_Δ values determined to be 0.021 for ZnPc(tomamine)$_1$, 0.0091 for ZnPc(tomamine)$_2$, 0.017 for ZnPc(tomamine)$_3$ and 0.0040 for ZnPc(tomamine)$_4$ (Figure S47).

$$\frac{\Phi_{Standard}}{\Phi_{Unknown}} = \frac{Slope\ from\ Stanards}{Slope\ from\ Unknowns}$$

Spectroscopy of compounds

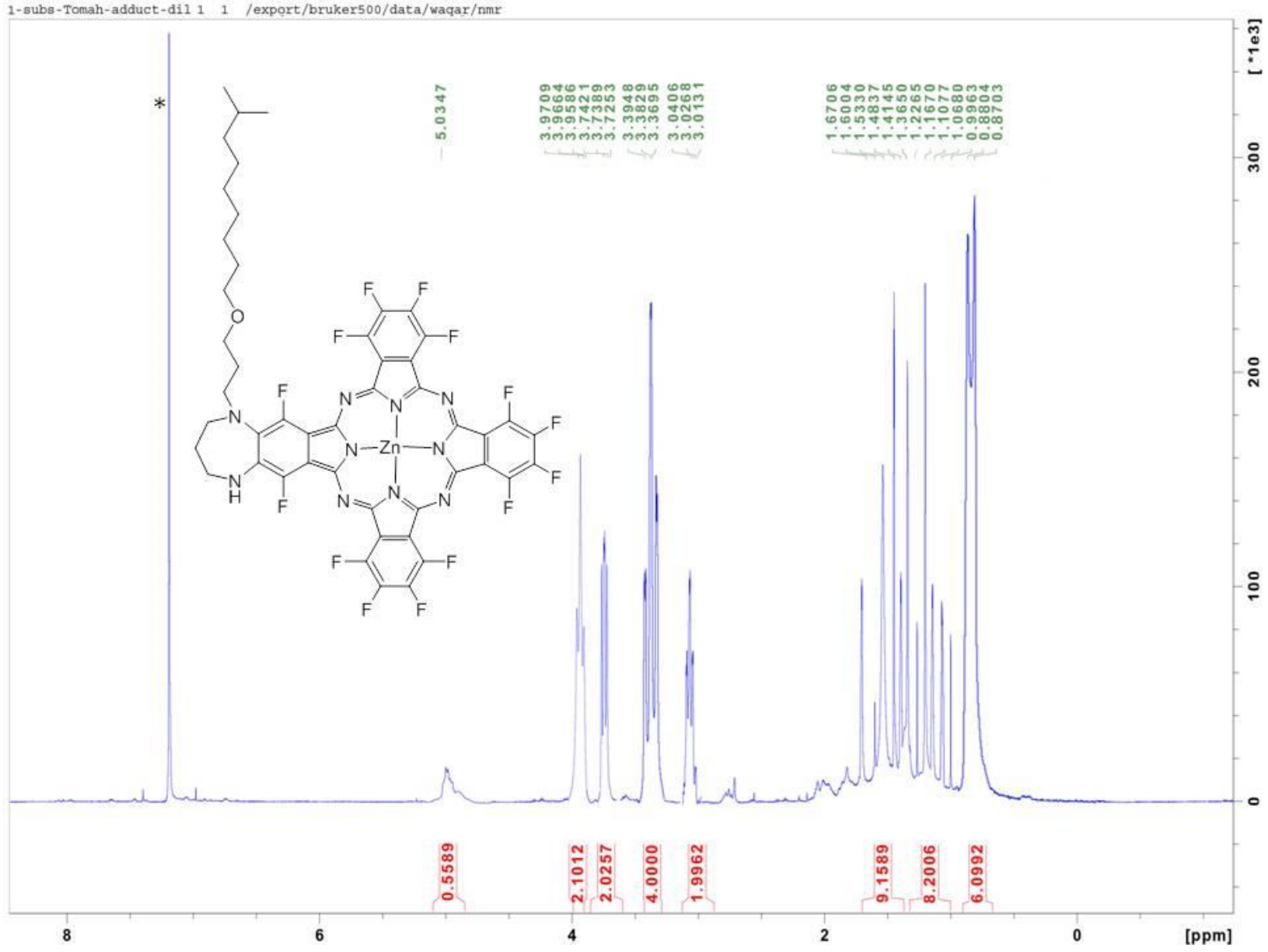

Figure S1. ^{1}H NMR of ZnPc(tomamine)$_1$ $CDCL_3$**.** * $CDCl_3$

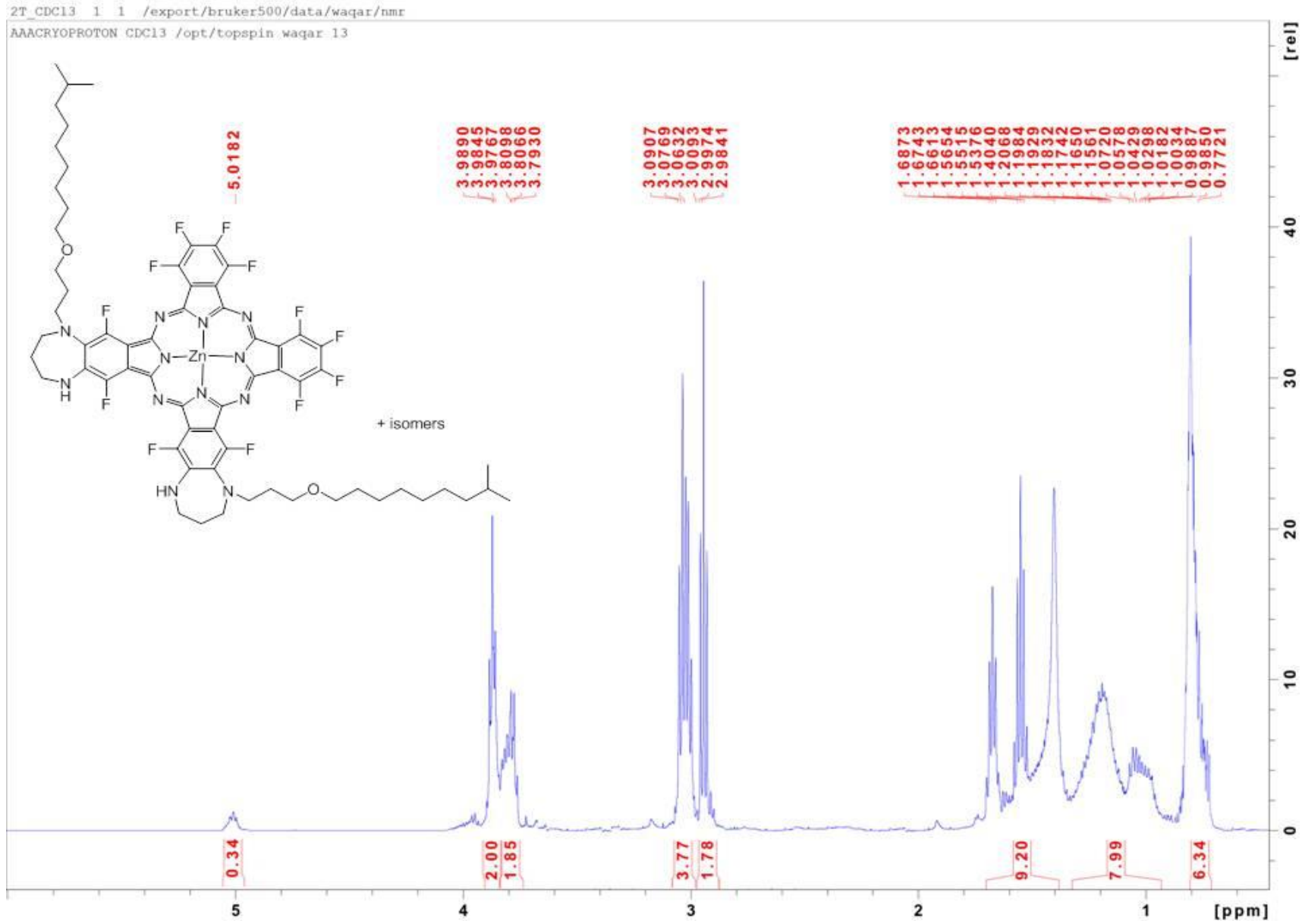

Figure S2. ^{1}H NMR of $ZnPc(tomamine)_2$ in $CDCl_3$**.**

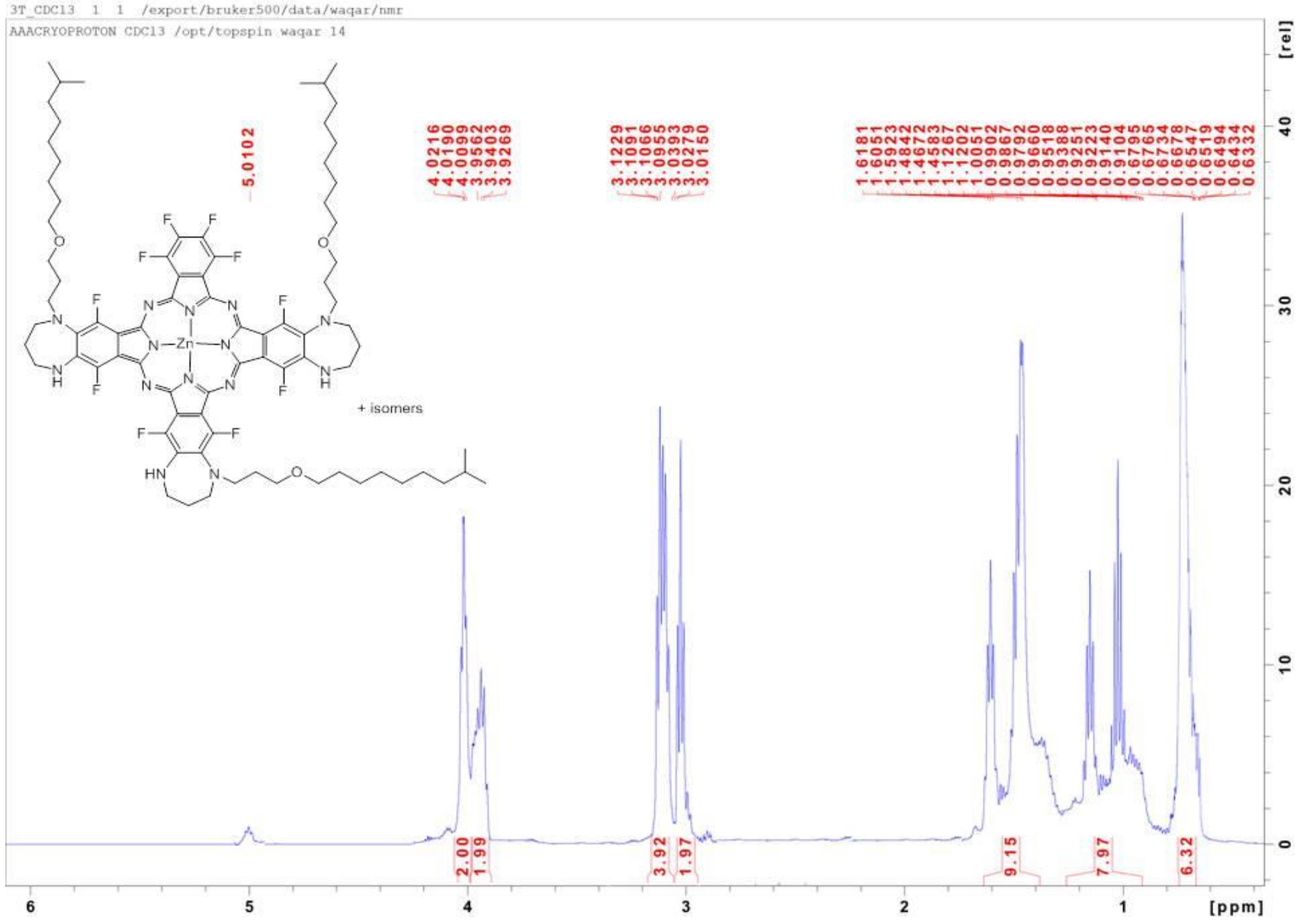

Figure S3. ^{1}H NMR of ZnPc(tomamine)$_3$ in $CDCl_3$.

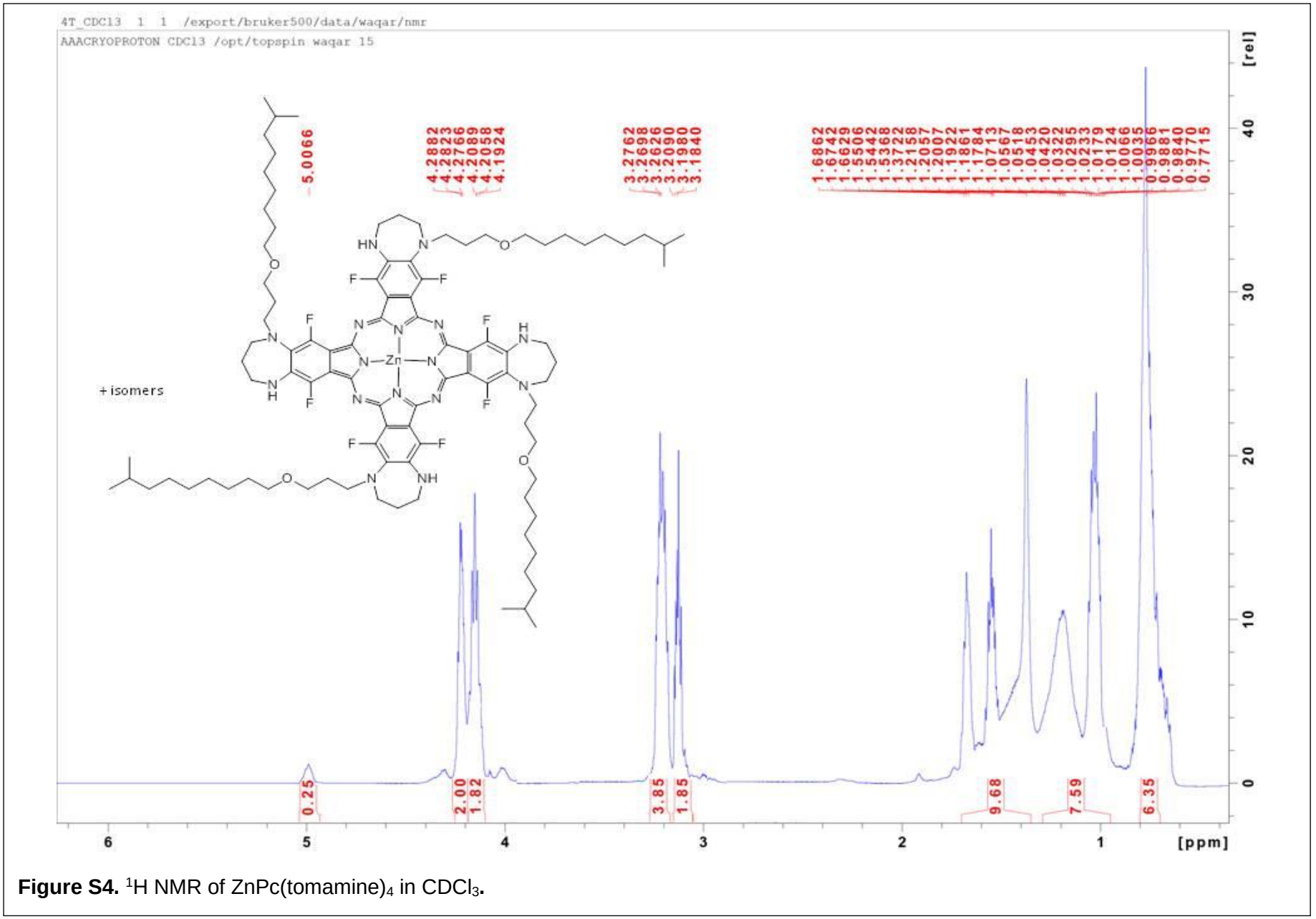

Figure S4. ^{1}H NMR of $ZnPc(tomamine)_4$ in $CDCl_3$**.**

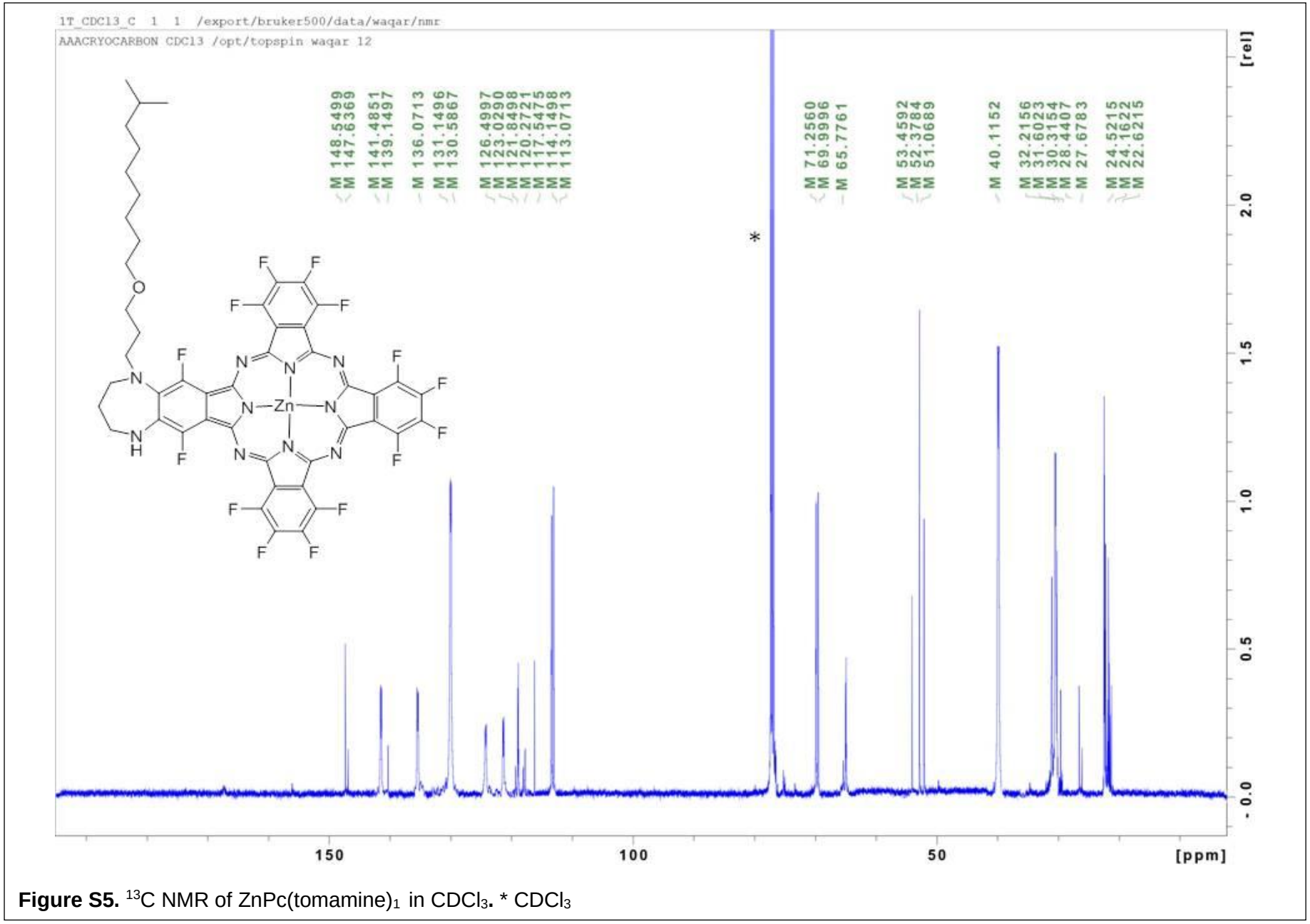

Figure S5. ^{13}C NMR of ZnPc(tomamine)$_1$ in $CDCl_3$**.** * $CDCl_3$

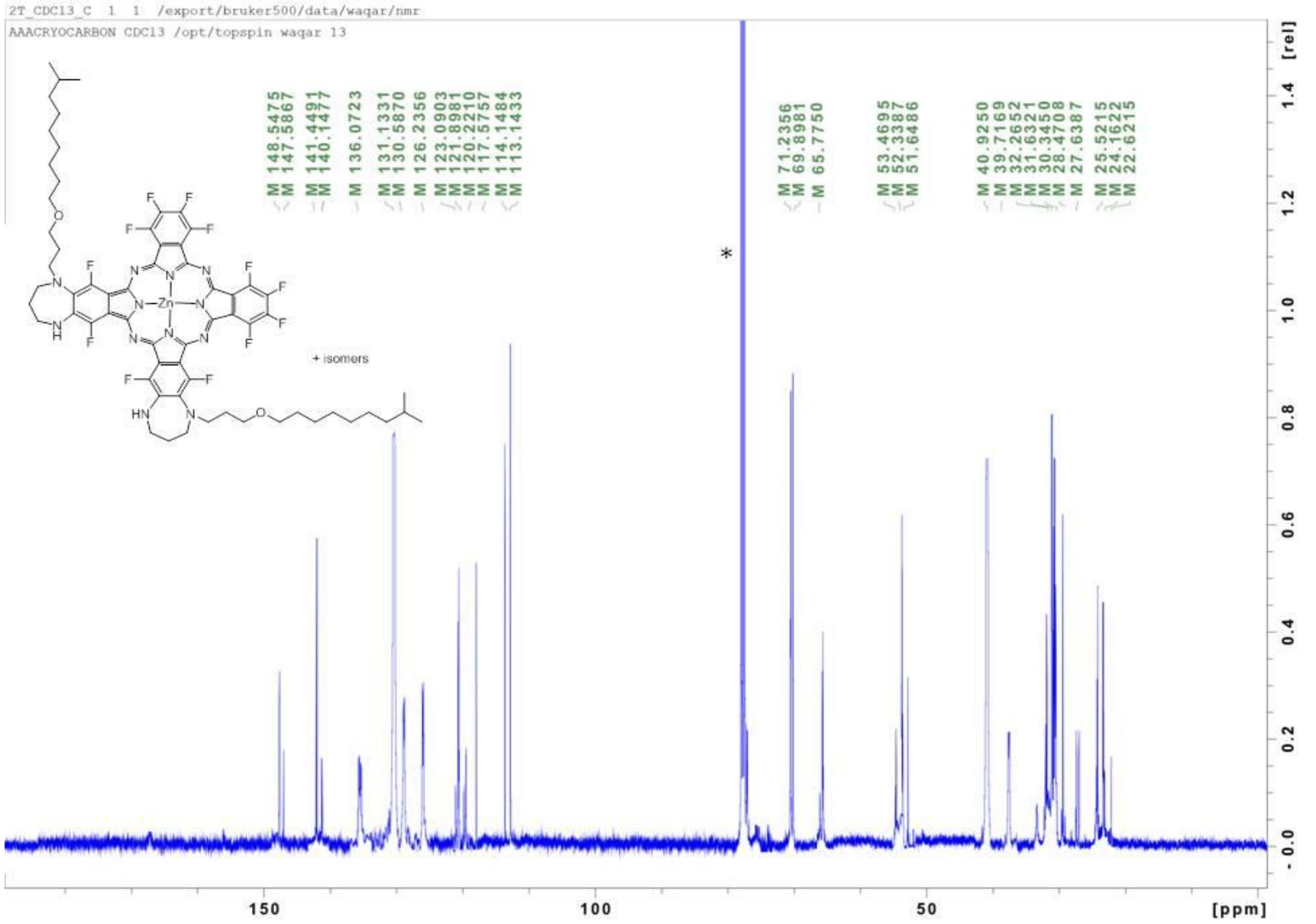

Figure S6. ^{13}C NMR of ZnPc(tomamine)$_2$ in $CDCl_3$**.** * $CDCl_3$

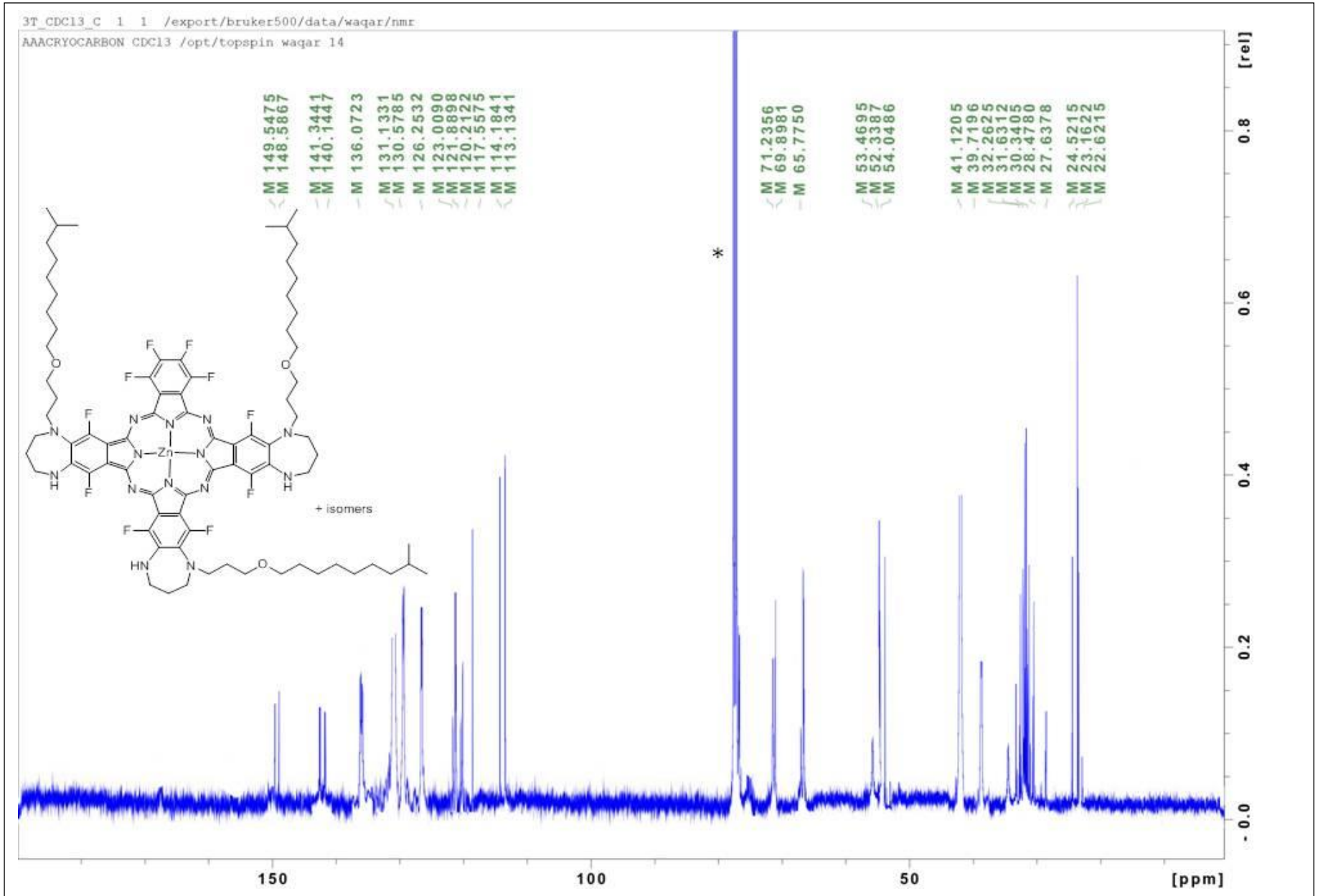

Figure S7. ^{13}C NMR of ZnPc(tomamine)$_3$ in $CDCl_3$**.** * $CDCl_3$

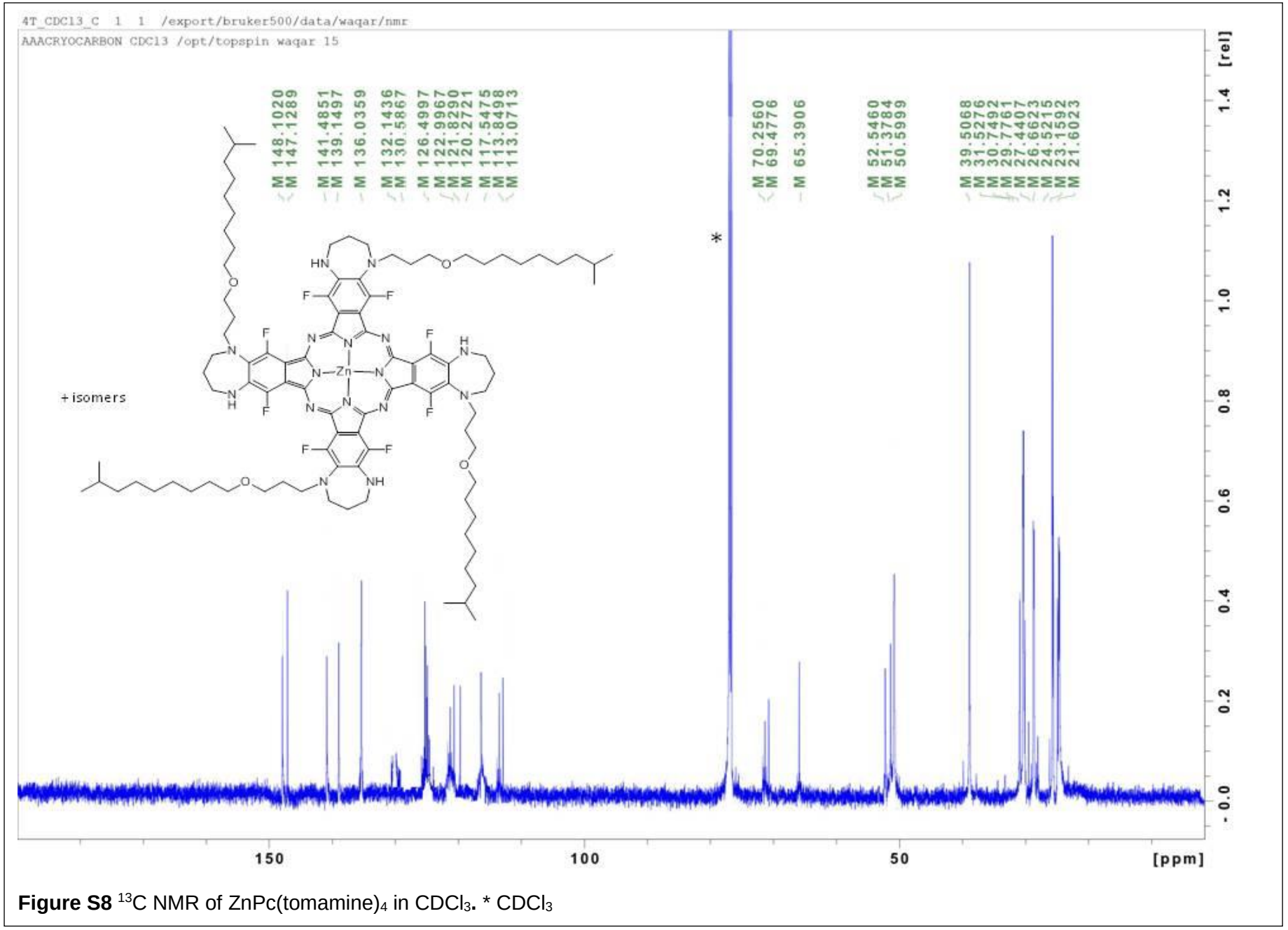

Figure S8 ^{13}C NMR of ZnPc(tomamine)$_4$ in $CDCl_3$**.** * $CDCl_3$

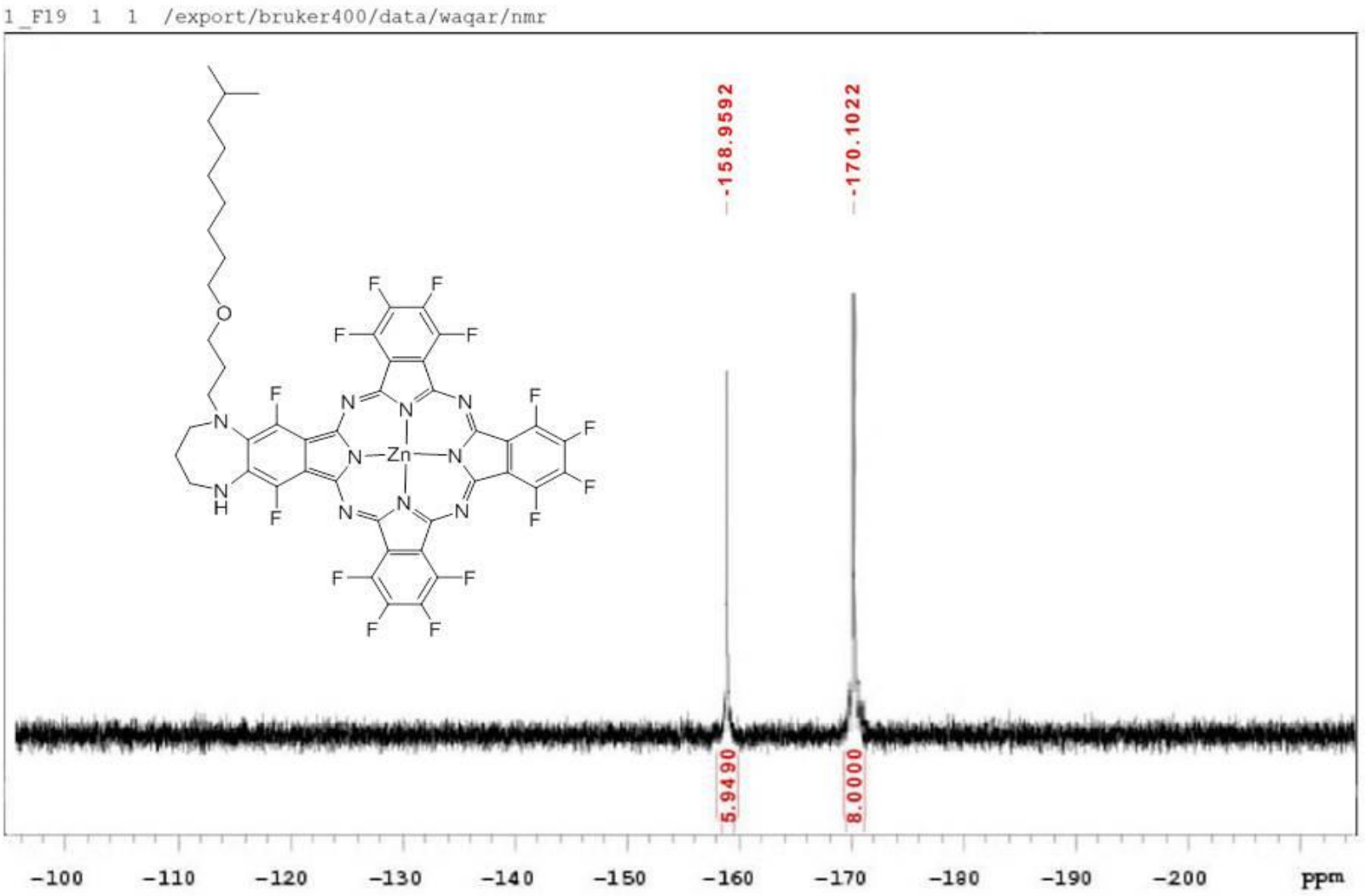

Figure S9. ^{19}F NMR of ZnPc(tomamine)$_1$ in $CDCl_3$.

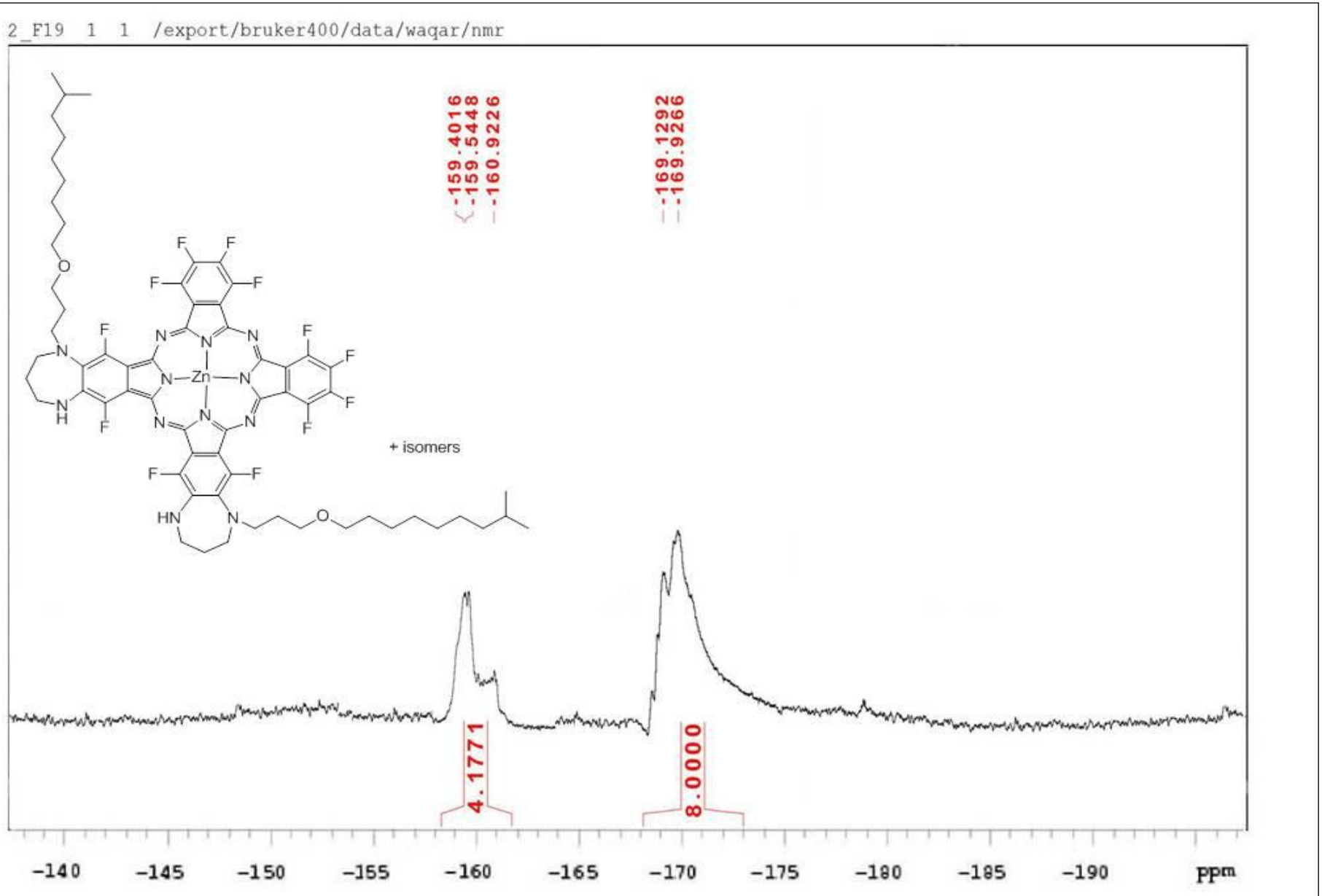

Figure S10. ^{19}F NMR of ZnPc(tomamine)$_2$ in $CDCl_3$.

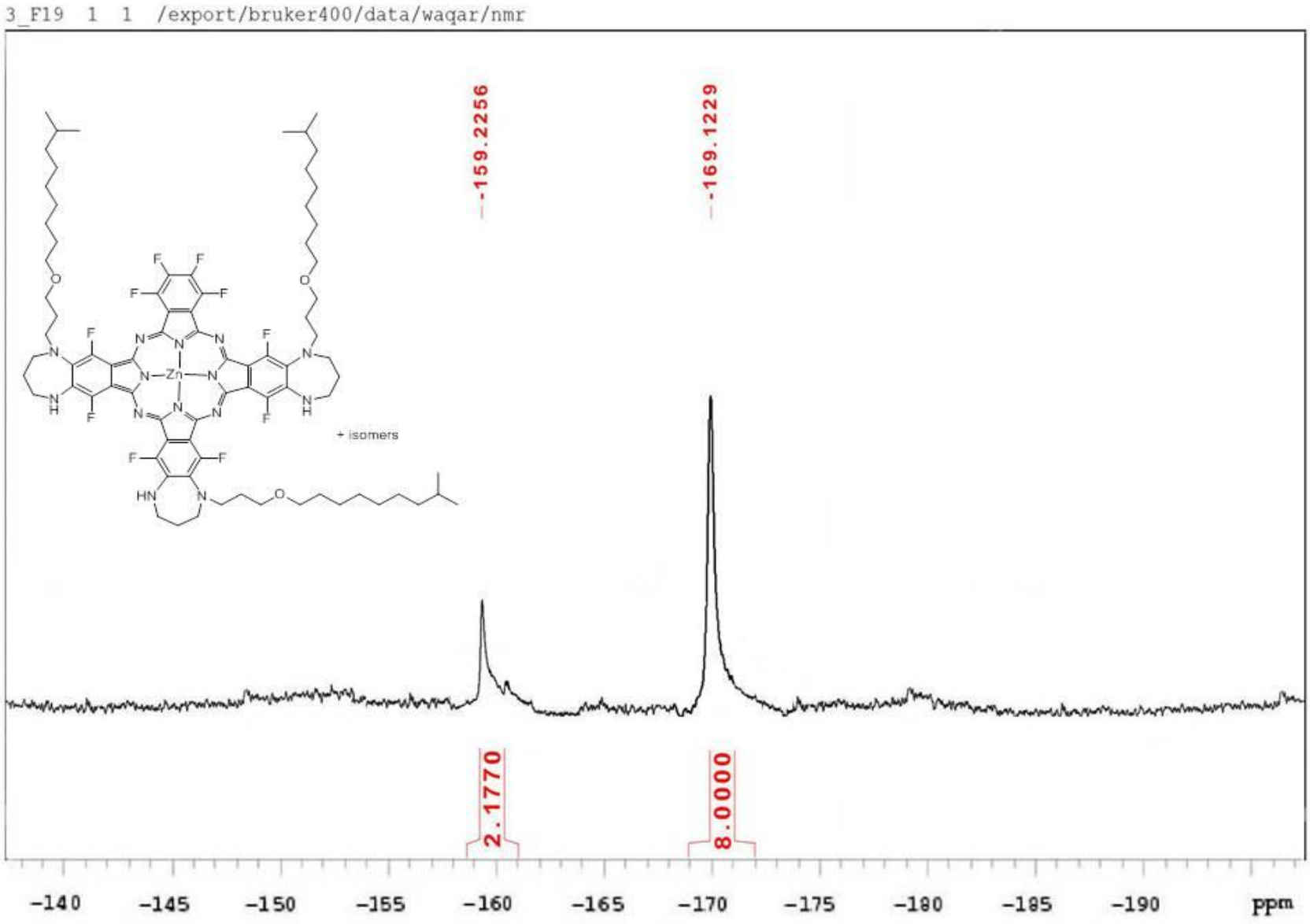

Figure S11. ^{19}F NMR of ZnPc(tomamine)$_3$ in $CDCl_3$.

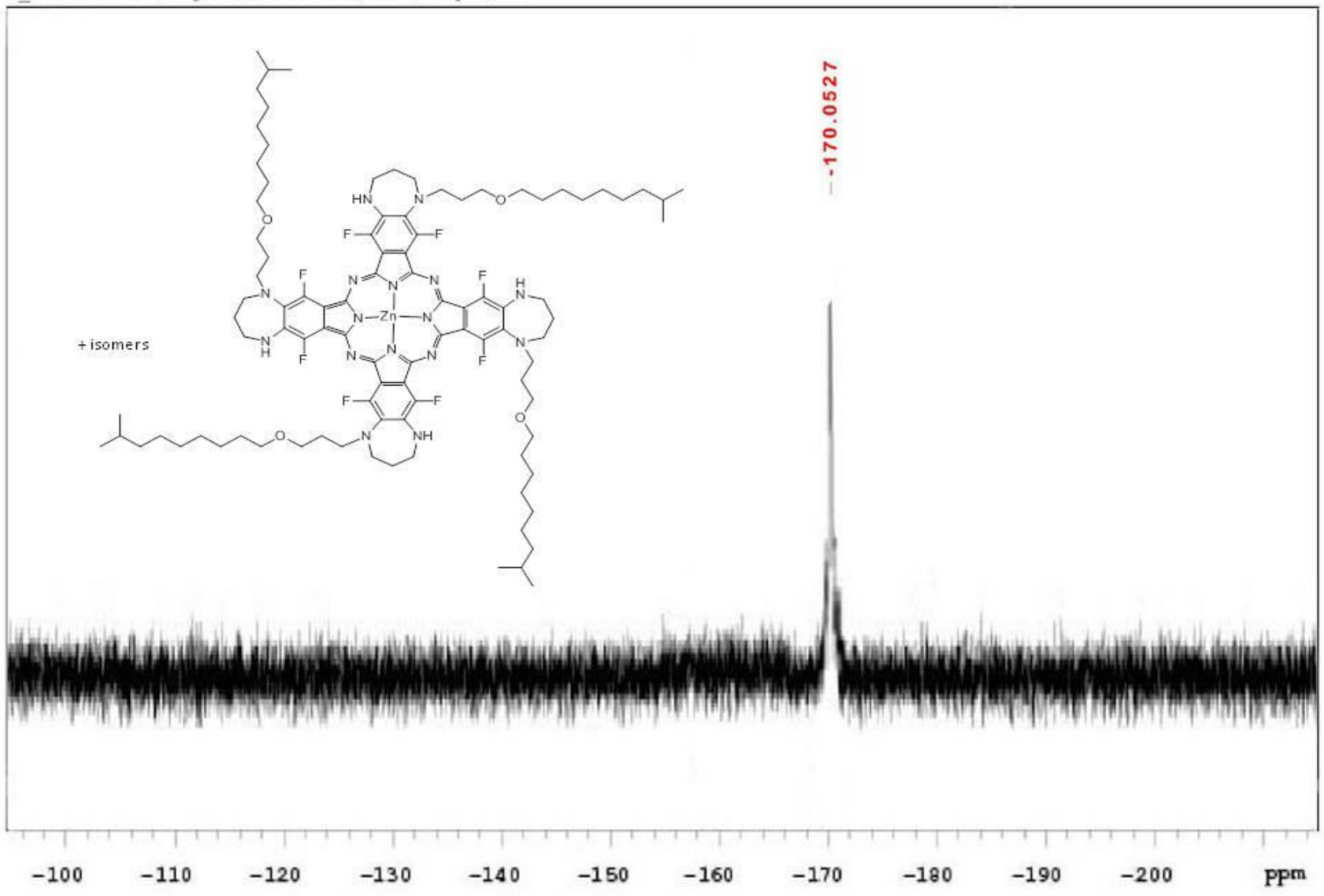

Figure S12. ^{19}F NMR of ZnPc(tomamine)$_4$ in $CDCl_3$.

Qualitative Compound Report

Compound Table

Compound Label	RT	Mass	Abund	Formula	Tgt Mass	Diff (ppm)	MFG Formula	DB Formula
Cpd 1: C48 H34 F14 N10 O Zn	0.075	1096.1968	2239	C48 H34 F14 N10 O Zn	1096.1985	-1.55	C48 H34 F14 N10 O Zn	C48 H34 F14 N10 O Zn

Compound Label	*m/z*	RT	Algorithm	Mass
Cpd 1: C48 H34 F14 N10 O Zn	1097.2058	0.075	Find By Formula	1096.1968

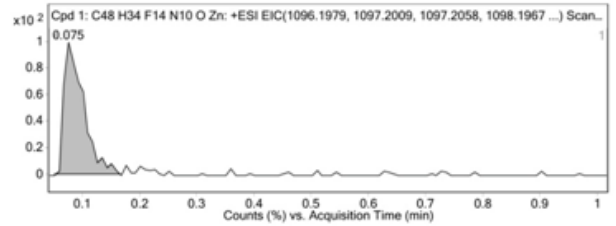

MS Spectrum

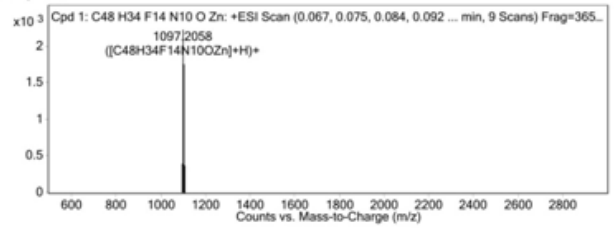

MS Zoomed Spectrum

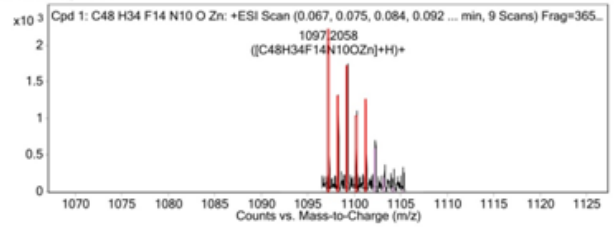

MS Spectrum Peak List

m/z	*Calc m/z*	Diff(ppm)	z	Abund	Formula	Ion
1097.2058	1097.2058	-0.03	1	2239.48	C48H34F14N10OZn	(M+H)+
1098.2071	1098.2087	1.52	1	1340.35	C48H34F14N10OZn	(M+H)+
1099.2023	1099.2046	2.06	1	1743.76	C48H34F14N10OZn	(M+H)+
1100.2035	1100.2059	2.13	1	1109.29	C48H34F14N10OZn	(M+H)+
1101.1998	1101.2033	3.14	1	1245.64	C48H34F14N10OZn	(M+H)+

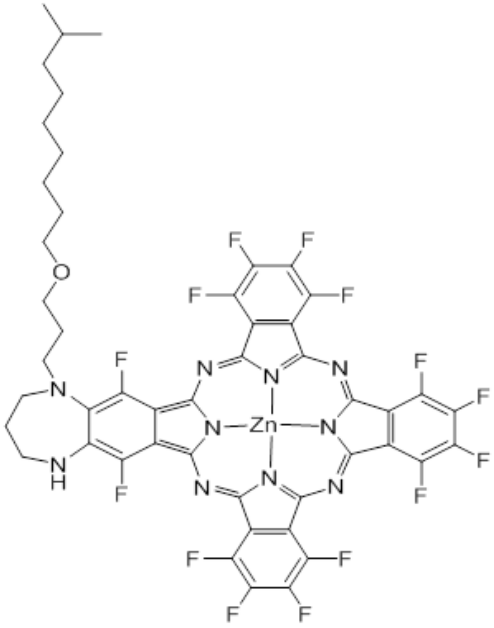

Agilent Technologies Page 1 of 1 Printed at: 11:35 AM on:10/27/2014

Figure S13. High resolution mass spectrum of compound ZnPc(tomamine)$_1$**.**

Qualitative Compound Report

Compound Table

Compound Label	RT	Mass	Abund	Formula	Tgt Mass	Diff (ppm)	MFG Formula	DB Formula
Cpd 1: C64 H68 F12 N12 O2 Zn	0.075	1328.4672	4847	C64 H68 F12 N12 O2 Zn	1328.4688	-1.18	C64 H68 F12 N12 O2 Zn	C64 H68 F12 N12 O2 Zn

Compound Label	*m/z*	RT	Algorithm	Mass
Cpd 1: C64 H68 F12 N12 O2 Zn	1329.4748	0.075	Find By Formula	1328.4672

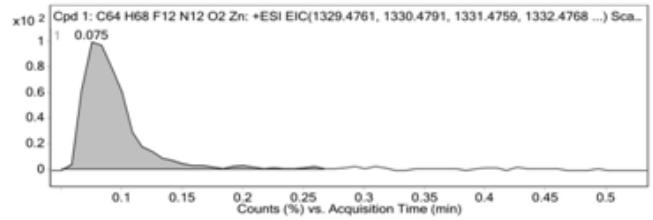

MS Spectrum

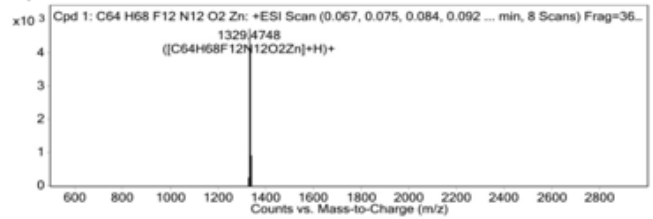

MS Zoomed Spectrum

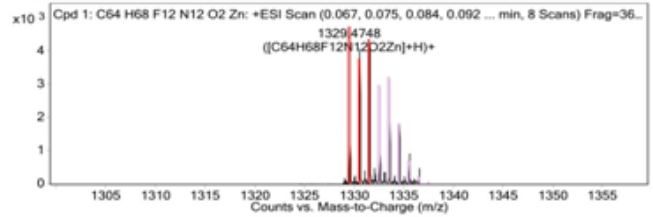

MS Spectrum Peak List

m/z	*Calc m/z*	Diff(ppm)	z	Abund	Formula	Ion
1329.4748	1329.4761	0.99	1	4847.38	C64H68F12N12O2Zn	(M+H)+
1330.4775	1330.4791	1.23	1	4168.3	C64H68F12N12O2Zn	(M+H)+
1331.4741	1331.4759	1.34	1	4163.32	C64H68F12N12O2Zn	(M+H)+

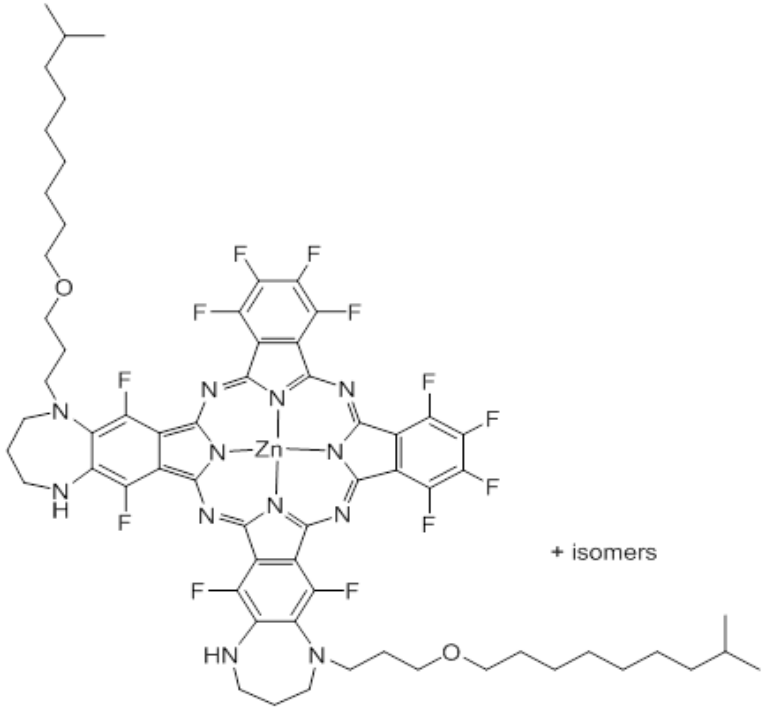

Agilent Technologies Page 1 of 1 Printed at: 12:28 PM on:10/17/2014

Figure S14. High resolution mass spectrum of compound ZnPc(tomamine)$_2$**.**

Qualitative Compound Report

Compound Table

Compound Label	RT	Mass	Abund	Formula	Tgt Mass	Diff (ppm)	MFG Formula	DB Formula
Cpd 1: C80 H102 F10 N14 O3 Zn	0.092	1560.7418	24031	C80 H102 F10 N14 O3 Zn	1560.7391	1.74	C80 H102 F10 N14 O3 Zn	C80 H102 F10 N14 O3 Zn

Compound Label	*m/z*	RT	Algorithm	Mass
Cpd 1: C80 H102 F10 N14 O3 Zn	1563.7464	0.092	Find By Formula	1560.7418

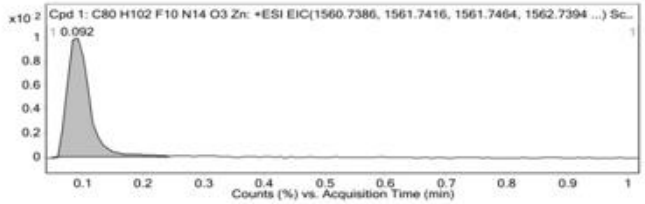

MS Spectrum

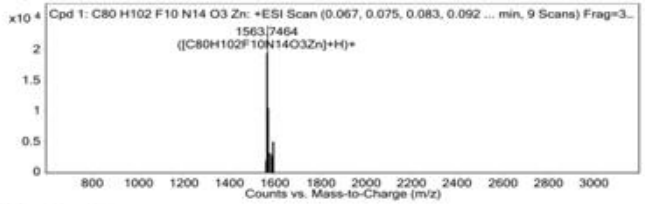

MS Zoomed Spectrum

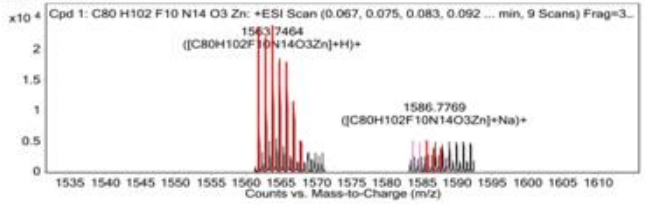

MS Spectrum Peak List

m/z	*Calc m/z*	Diff(ppm)	z	Abund	Formula	Ion
1561.7447	1561.7464	1.1	1	20378.73	C80H102F10N14O3Zn	(M+H)+
1562.7475	1562.7494	1.21	1	22566.97	C80H102F10N14O3Zn	(M+H)+
1563.7464	1563.7472	0.54	1	24030.79	C80H102F10N14O3Zn	(M+H)+
1564.7465	1564.7477	0.8	1	19062.35	C80H102F10N14O3Zn	(M+H)+
1565.7441	1565.7457	1.06	1	16620.76	C80H102F10N14O3Zn	(M+H)+
1566.7441	1566.7469	1.77	1	10721.53	C80H102F10N14O3Zn	(M+H)+
1567.7427	1567.7488	3.86	1	5287.1	C80H102F10N14O3Zn	(M+H)+
1585.7556	1585.7291	-16.69	1	3007.11	C80H102F10N14O3Zn	(M+Na)+
1586.7769	1586.7297	-29.8	1	5134.8	C80H102F10N14O3Zn	(M+Na)+
1587.7801	1587.7277	-33.04	1	4672.13	C80H102F10N14O3Zn	(M+Na)+

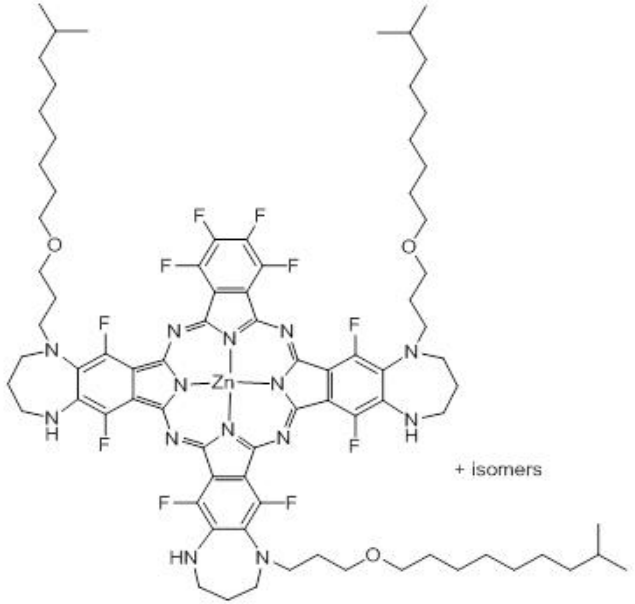

Agilent Technologies

Page 1 of 1

Printed at: 3:40 PM on:11/11/2014

Figure S15. High resolution mass spectrum of compound ZnPc(tomamine)$_3$**.**

Qualitative Compound Report

Compound Table

Compound Label	RT	Mass	Abund	Formula	Tgt Mass	Diff (ppm)	MFG Formula	DB Formula
Cpd 1: C96 H136 F8 N16 O4 Zn	0.081	1792.9961	2157	C96 H136 F8 N16 O4 Zn	1793.0094	-7.42	C96 H136 F8 N16 O4 Zn	C96 H136 F8 N16 O4 Zn

Compound Label	*m/z*	RT	Algorithm	Mass
Cpd 1: C96 H136 F8 N16 O4 Zn	1818.0035	0.081	Find By Formula	1792.9961

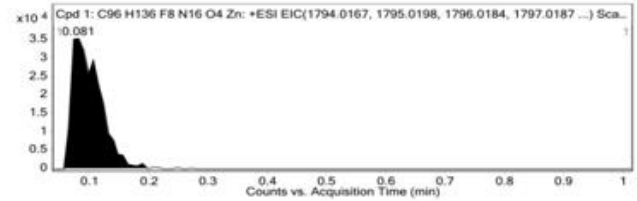

MS Spectrum

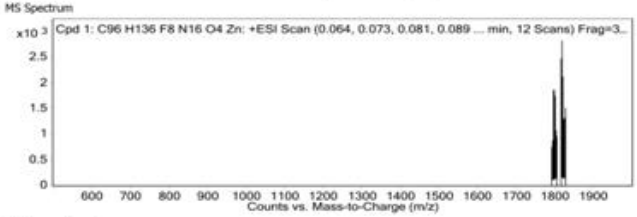

MS Zoomed Spectrum

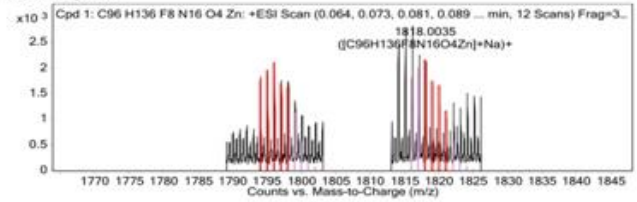

MS Spectrum Peak List

m/z	*Calc m/z*	Diff(ppm)	z	Abund	Formula	Ion
1793.991	1794.0167	14.33	1	1813.94	C96H136F8N16O4Zn	(M+H)+
1794.9966	1795.0198	12.88	1	1844.15	C96H136F8N16O4Zn	(M+H)+
1795.9958	1796.0184	12.59	1	1878.71	C96H136F8N16O4Zn	(M+H)+
1796.9944	1797.0187	13.53	1	1780.11	C96H136F8N16O4Zn	(M+H)+
1797.992	1798.017	13.9	1	1768.46	C96H136F8N16O4Zn	(M+H)+
1818.0035	1818.0003	-1.78	1	2157.11	C96H136F8N16O4Zn	(M+Na)+
1819.0056	1819.0006	-2.73	1	1719.79	C96H136F8N16O4Zn	(M+Na)+
1819.9997	1819.9989	-0.41	1	1327.19	C96H136F8N16O4Zn	(M+Na)+
1820.9997	1820.9997	0.01	1	938.65	C96H136F8N16O4Zn	(M+Na)+

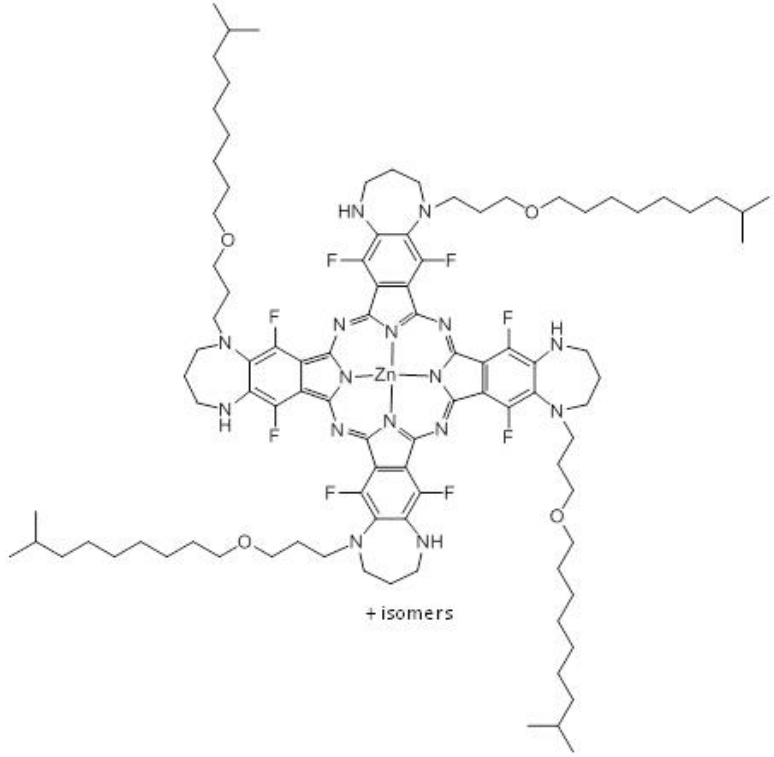

Agilent Technologies Page 1 of 1 Printed at: 12:49 PM on:4/21/2015

Figure S16. High resolution mass spectrum of compound ZnPc(tomamine)$_4$**.**

Solvent Dependence

Compound	Solvent	Dipole moment[a]	Dielectric constant[a]	UV-visible Absorption λ_{max}(log ε)	$^1O_2$ Φ_Δ[b]	Aggr. Size (nm)
ZnPc(tomamine)$_1$	Acetone	2.9 D	20.6	347, 674, 745 (3.51)	0.019	53
	DCM	1.8 D	9.1	348, 690, 747 (3.38)	-	-
	MeOH	1.7 D	32.6	347, 700, 754 (2.74)	-	-
	PBS	1.87 D	79.7	348, 690, 755 (2.65)	-	89
	THF	1.75 D	7.6	348, 656, 754 (3.70)	-	-
	DMSO	3.96 D	46.6	347, 700, 774 (3.60)	-	-
ZnPc(tomamine)$_2$	Acetone			348, 730, 768 (3.45)	0.009	69
	DCM			349, 732, 770 (3.38)	-	-
	MeOH			348, 710, 795 (2.57)	-	-
	PBS			349, 730, 768 (2.49)	-	133
	THF			349, 731, 767 (3.62)	-	-
	DMSO			348, 735, 810 (3.49)	-	-
ZnPc(tomamine)$_3$	Acetone			350, 690, 778 (3.39)	0.016	98
	DCM			351, 702, 784 (3.41)	-	-
	MeOH			350, 710, 786 (2.50)	-	-
	PBS			350, 705, 790 (2.39)	-	193
	THF			351, 702, 787 (3.54)	-	-
	DMSO			350, 715, 805 (3.38)	-	-
ZnPc(tomamine)$_4$	Acetone			354, 702, 795 (3.42)	0.004	122
	DCM			355, 716, 809 (3.36)	-	-
	MeOH			354, 725, 805 (2.43)	-	-
	PBS			355, 710, 802 (2.21)	-	223
	THF			355, 708, 804 (3.56)	-	-
	DMSO			355, 726, 820 (3.25)	-	-

Table S3. Solvent dependence of UV-visible, $^1O_2$ Φ_Δ and aggregation of ZnPc(tomamine)$_1$, ZnPc(tomamine)$_2$, ZnPc(tomamine)$_3$, and ZnPc(tomamine)$_4$. UV-visible spectra are given below. [a] Handbook of solvent properties,[1] [b] acetone-d_6

Note: aggregation of these dyes is solvent and concentration dependent, thus for all spectra and experiments concentrations were chosen to avoid aggregation of the dyes.

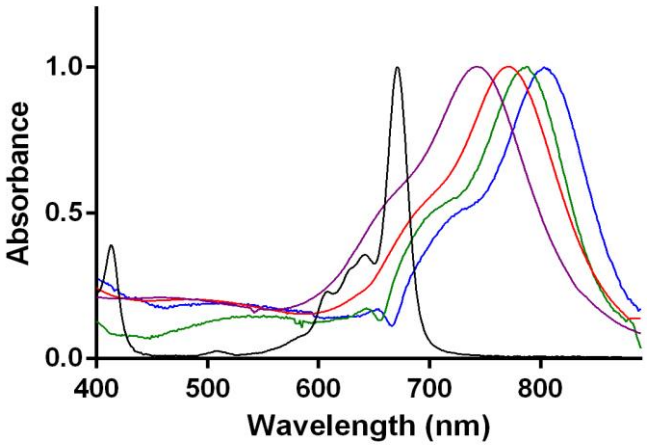

Figure S17. UV-visible absorbance spectra of compounds $ZnF_{16}Pc$ (black), $ZnPc(tomamine)_1$ (pink), $ZnPc(tomamine)_2$ (red), $ZnPc(tomamine)_3$ (green) and $ZnPc(tomamine)_4$ (blue) in THF.

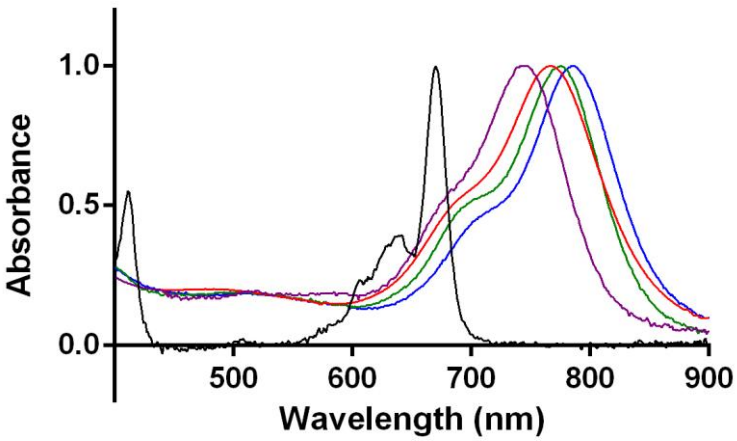

Figure S18. UV-visible absorbance spectra of compounds $ZnF_{16}Pc$ (black), $ZnPc(tomamine)_1$ (pink), $ZnPc(tomamine)_2$ (red), $ZnPc(tomamine)_3$ (green) and $ZnPc(tomamine)_4$ (blue) in acetone.

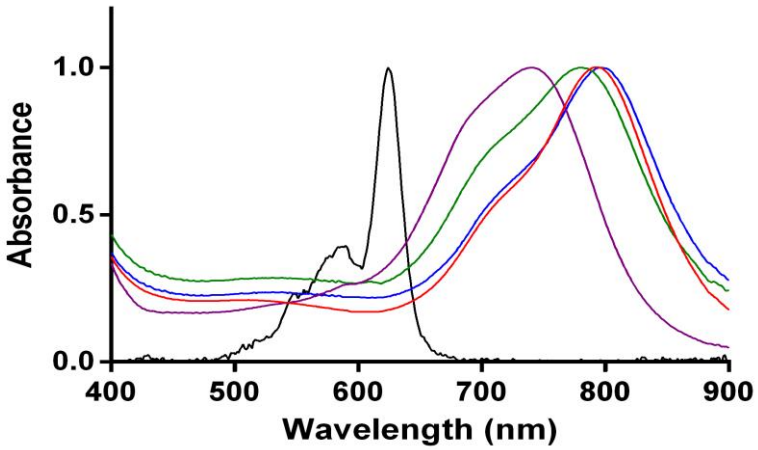

Figure S19. UV-visible absorbance spectra of compounds $ZnF_{16}Pc$ (black), $ZnPc(tomamine)_1$ (pink), $ZnPc(tomamine)_2$ (red), $ZnPc(tomamine)_3$ (green) and $ZnPc(tomamine)_4$ (blue) in CH_2Cl_2.

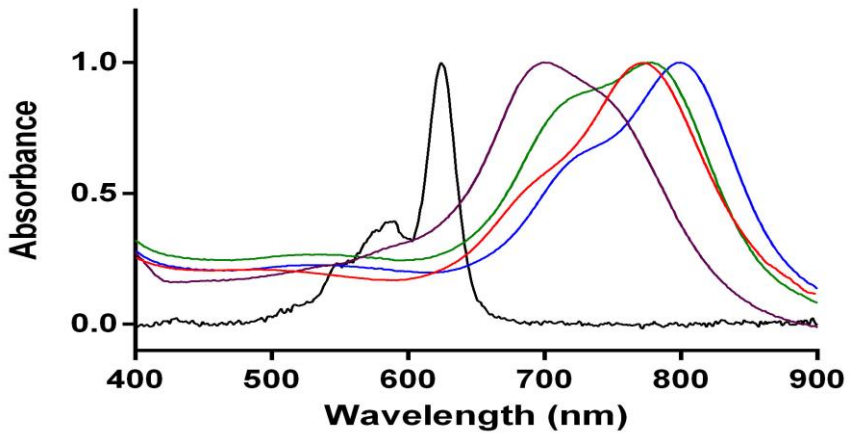

Figure S20. UV-visible absorbance spectra of compounds $ZnF_{16}Pc$ (black), $ZnPc(tomamine)_1$ (pink), $ZnPc(tomamine)_2$ (red), $ZnPc(tomamine)_3$ (green) and $ZnPc(tomamine)_4$ (blue) in MeOH.

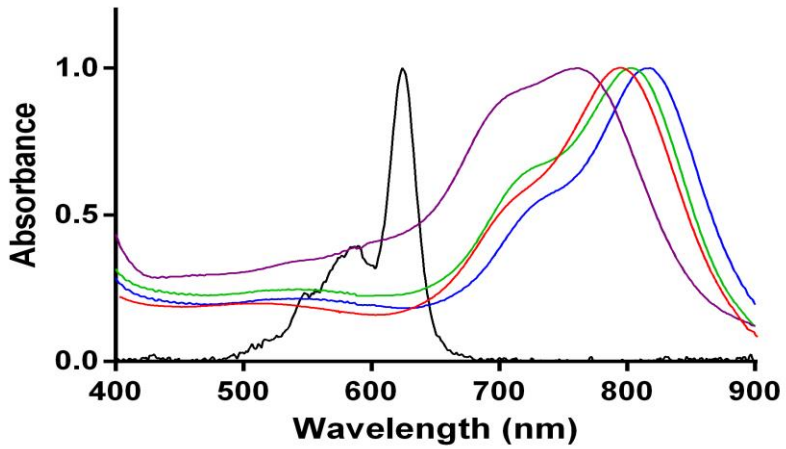

Figure S21. UV-visible absorbance spectra of compounds $ZnF_{16}Pc$ (black), $ZnPc(tomamine)_1$ (pink), $ZnPc(tomamine)_2$ (red), $ZnPc(tomamine)_3$ (green) and $ZnPc(tomamine)_4$ (blue) in DMSO.

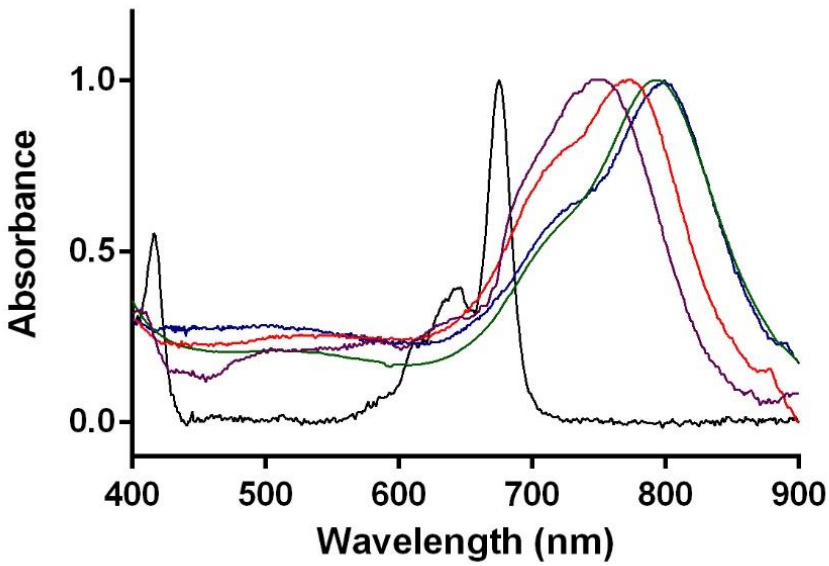

Figure S22. UV-visible absorbance spectra of compounds $ZnF_{16}Pc$ (black), $ZnPc(tomamine)_1$ (pink), $ZnPc(tomamine)_2$ (red), $ZnPc(tomamine)_3$ (green) and $ZnPc(tomamine)_4$ (blue) in PBS.

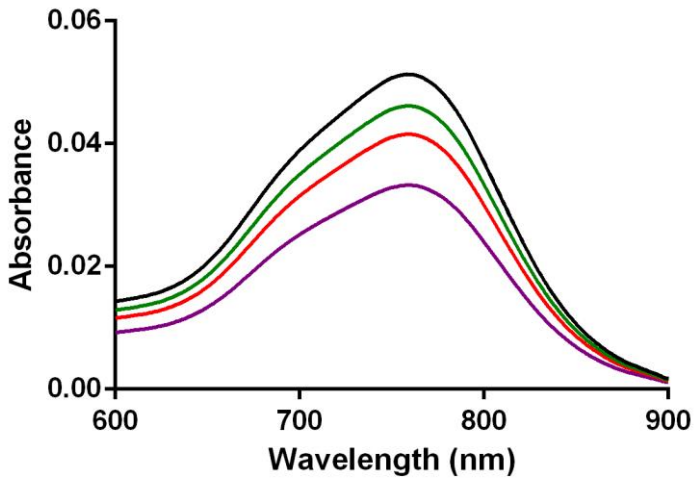

Figure S23. Photostability study of ZnPc(tomamine)$_1$. UV-visible absorbance spectra taken using 1 cm glass cuvette in acetone at time = 0 h (black), 2 h (green), 4 h (red) and 8 h (purple). Exposed under direct 13 W white light bulb at 0.41 mW/cm^2.

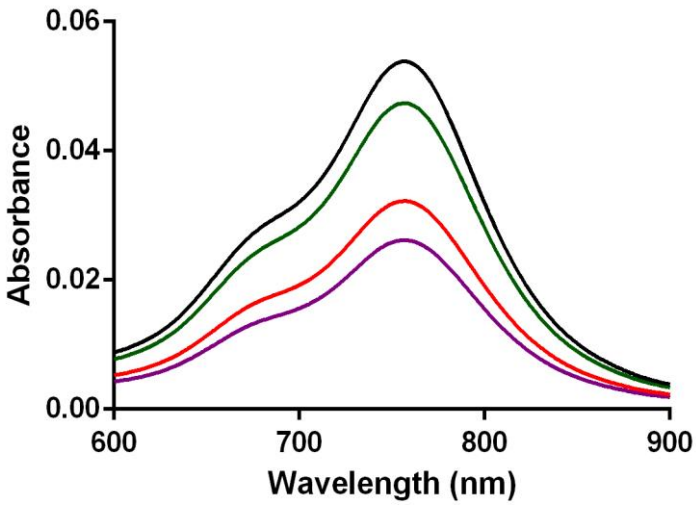

Figure S24. Photostability study of compound ZnPc(tomamine)$_2$. UV-visible absorbance spectra taken using 1 cm glass cuvette in acetone at time = 0 h (black), 2 h (green), 4 h (red) and 8 h (purple). Exposed under direct 13 W white light bulb at 0.41 mW/cm^2.

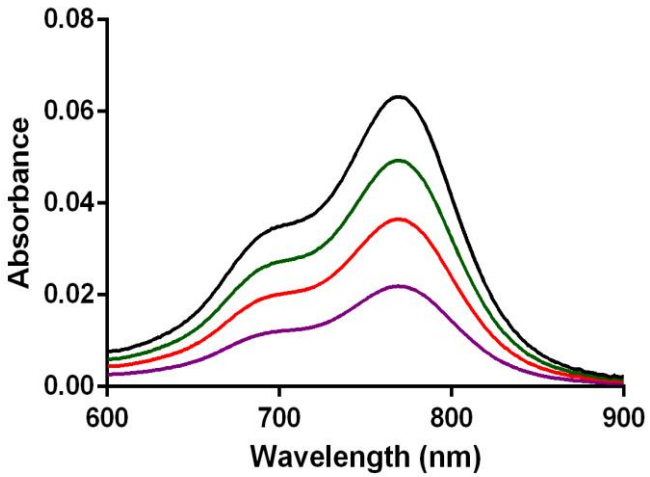

Figure S25. Photostability study of compound ZnPc(tomamine)$_3$. UV-visible absorbance spectra taken using 1 cm glass cuvette in acetone at time = 0 h (black), 2 h (green), 4 h (red) and 8 h (purple). Exposed under direct 13 W white light bulb at 0.41 mW/cm^2.

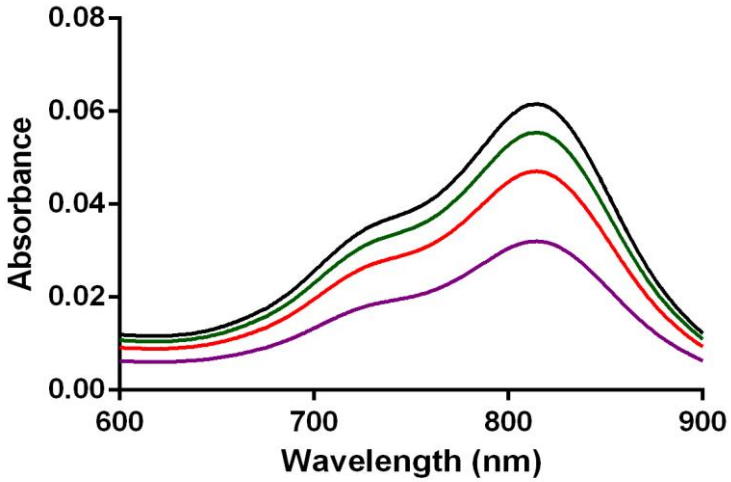

Figure S26. Photostability study of compound ZnPc(tomamine)$_4$. UV-visible absorbance spectra taken using 1 cm glass cuvette in acetone at time = 0 h (black), 2 h (green), 4 h (red) and 8 h (purple). Exposed under direct 13 W white fluorescent lamp at 0.41 mW/cm^2.

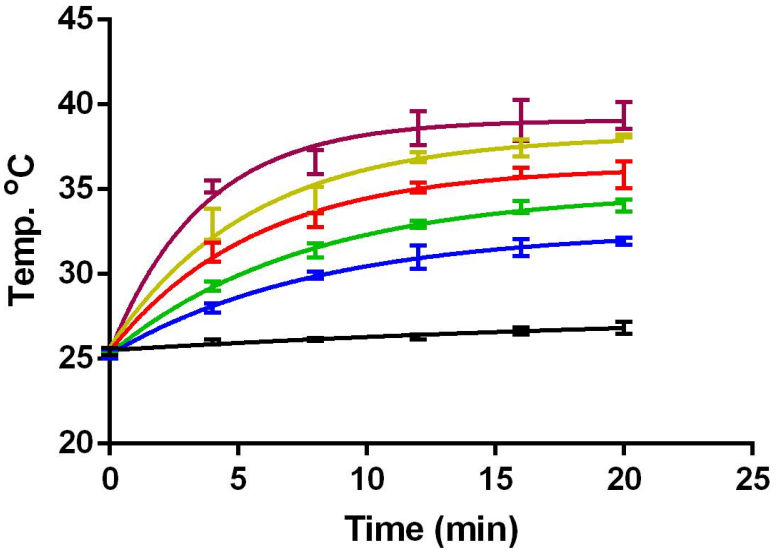

Figure S27. Photothermal study of ZnPc(tomamine)$_1$. Temperature taken using a digital thermometer of 0 µM (black), 20 µM (blue), 40 µM (green), 60 µM (red), 80 µM (yellow) and 100 µM (purple) of 1.5 mL solutions in PBS. Exposed under direct 13 W white fluorescent lamp at 0.92 mW/cm^2.

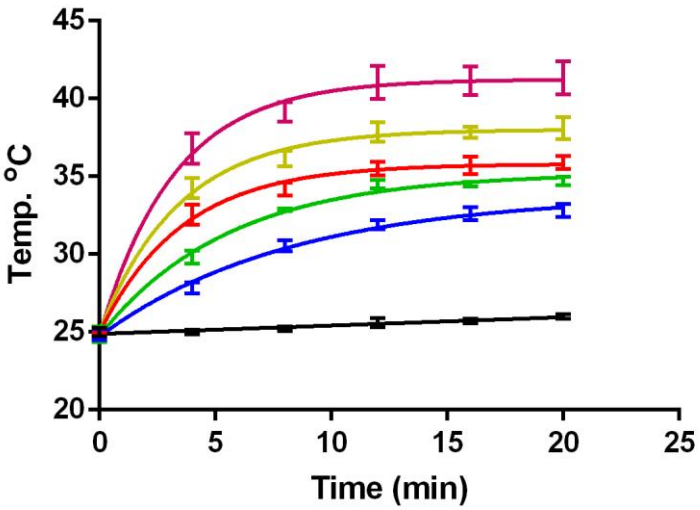

Figure S28. Photothermal study of ZnPc(tomamine)$_2$. Temperature taken using a digital thermometer of 0 µM (black), 20 µM (blue), 40 µM (green), 60 µM (red), 80 µM (yellow) and 100 µM (purple) 1.5 mL solutions in PBS. Exposed under direct 13 W white fluorescent lamp at 0.92 mW/cm^2.

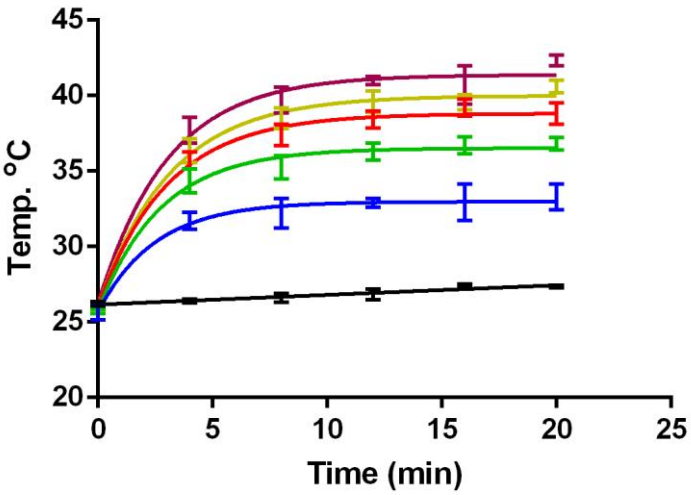

Figure S29. Photothermal study of ZnPc(tomamine)$_3$. Temperature taken using a digital thermometer of 0 µM (black), 20 µM (blue), 40 µM (green), 60 µM (red), 80 µM (yellow) and 100 µM (purple) 1.5 mL solutions in PBS. Exposed under direct 13 W white fluorescent lamp at 0.92 mW/cm^2.

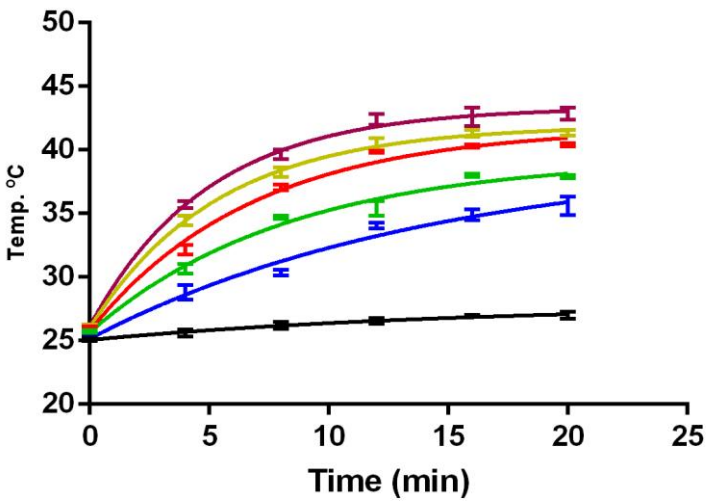

Figure S30. Photothermal study of ZnPc(tomamine)$_4$. Temperature taken using a digital thermometer of 0 µM (black), 20 µM (blue), 40 µM (green), 60 µM (red), 80 µM (yellow) and 100 µM (purple) 1.5 mL solutions in PBS. Exposed under direct 13 W white fluorescent lamp at 0.92 mW/cm^2.

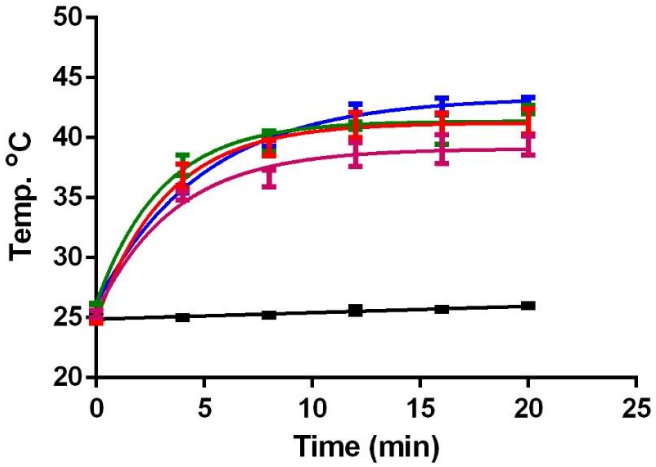

Figure S31. Overlay of photothermal studies of ZnPc(tomamine)$_1$ (pink), ZnPc(tomamine)$_2$ (red), ZnPc(tomamine)$_3$ (green) ZnPc(tomamine)$_4$ (blue) and no compound control (black) 1.5 mL solutions in PBS. Temperature taken every 4 min using a digital thermometer. 100 µM solutions were exposed under direct 13 W white fluorescent lamp at 0.92 mW/cm^2.

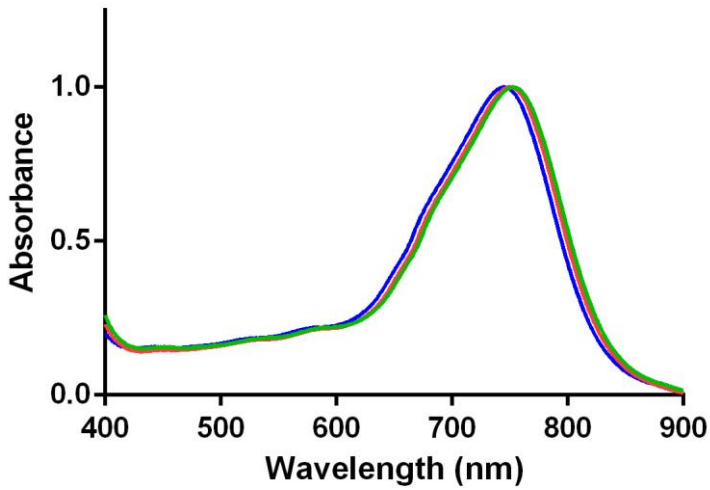

Figure S32. Overlay of temperature dependence UV-visible absorbance spectra of ZnPc(tomamine)$_1$ **at 0 ºC** (blue), 25 ºC (red) and 60 ºC (green) in THF.

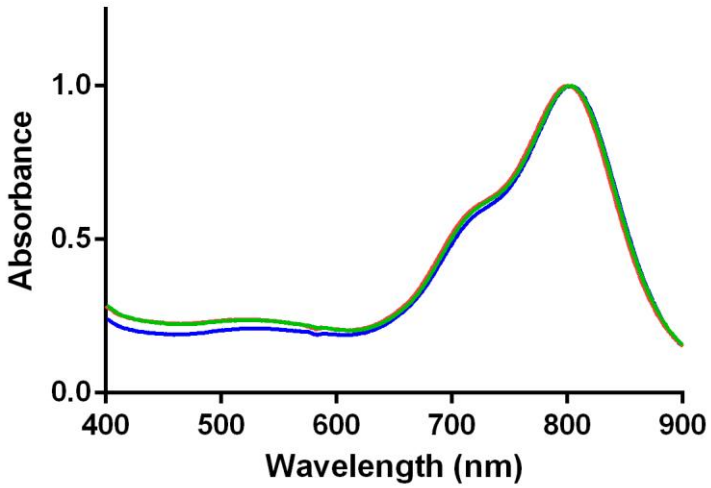

Figure S33. Overlay of temperature dependence UV-visible absorbance spectra of ZnPc(tomamine)$_4$ **at 0 ºC** (blue), 25 ºC (red) and 60 ºC (green) in THF.

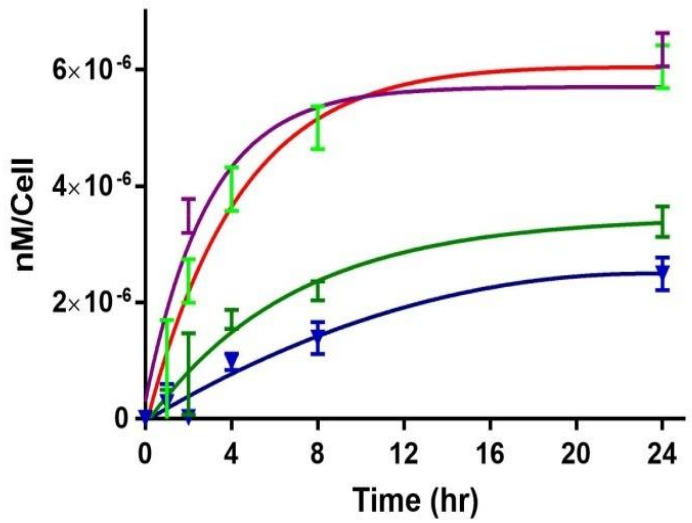

Figure S34. Uptake studies of ZnPc(tomamine)$_1$ (pink), ZnPc(tomamine)$_2$ (red), ZnPc(tomamine)$_3$ (green) and ZnPc(tomamine)$_4$ (blue) using MDA-MD231 breast cancer cells.

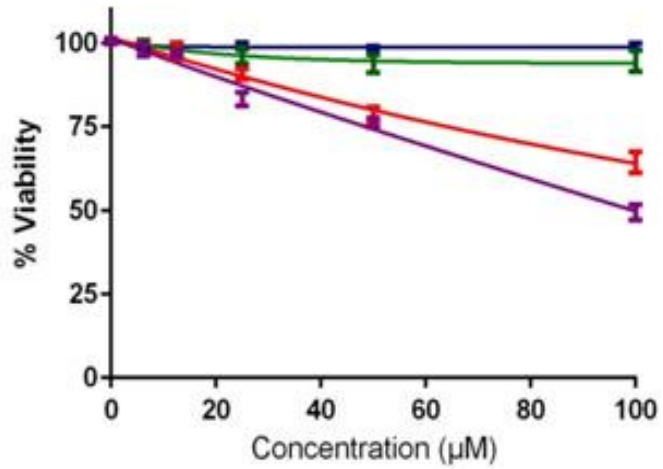

Figure S35. Dark toxicity studies of compounds ZnPc(tomamine)$_1$ (pink), ZnPc(tomamine)$_2$ (red), ZnPc(tomamine)$_3$ (green) and ZnPc(tomamine)$_4$ (blue)using MDA-MD231 breast cancer cells.

Compound	Octanol:PBS	$logP_{Oct:PBS}$
ZnPc(tomamine)$_1$	22:1	1.34
ZnPc(tomamine)$_2$	39:1	1.59
ZnPc(tomamine)$_3$	88:1	1.94
ZnPc(tomamine)$_4$	91:1	1.96

Table S4. Octanol/PBS partition coefficients.

Octanol-water partition coefficient values were determined for all four compounds using the shake flask method.[6] Data show that the log P increase and that solubility in aqueous media decreases with the number of tomamines added to the $ZnF_{16}Pc$. The dynamic light scattering (DLS) indicates these compounds form aggregates in phosphate buffered saline (PBS), where smaller aggregates were observed for mono and di substituted products when compared to tri and tetra substituted compounds (Figure S34-S37).

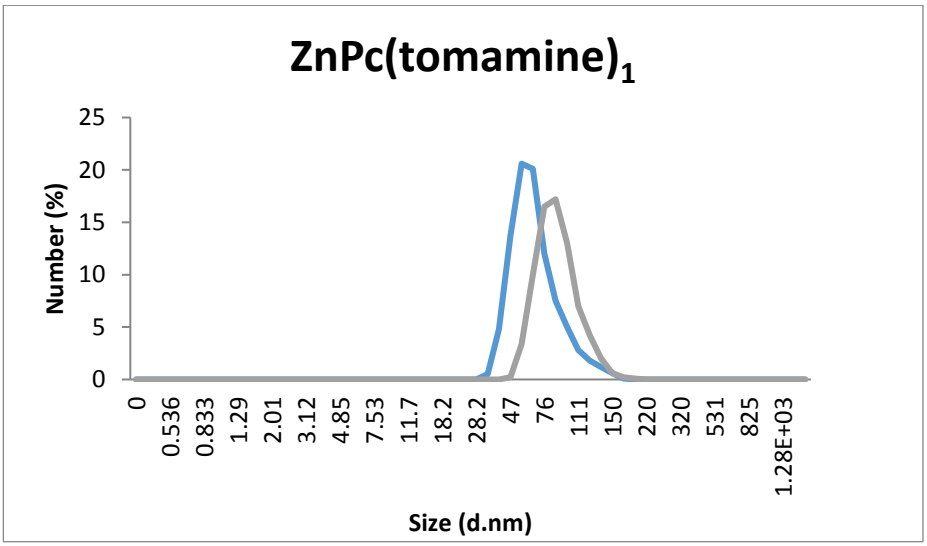

Figure S36. DLS of ZnPc(tomamine)$_1$ in acetone (blue) and PBS buffer (gray).

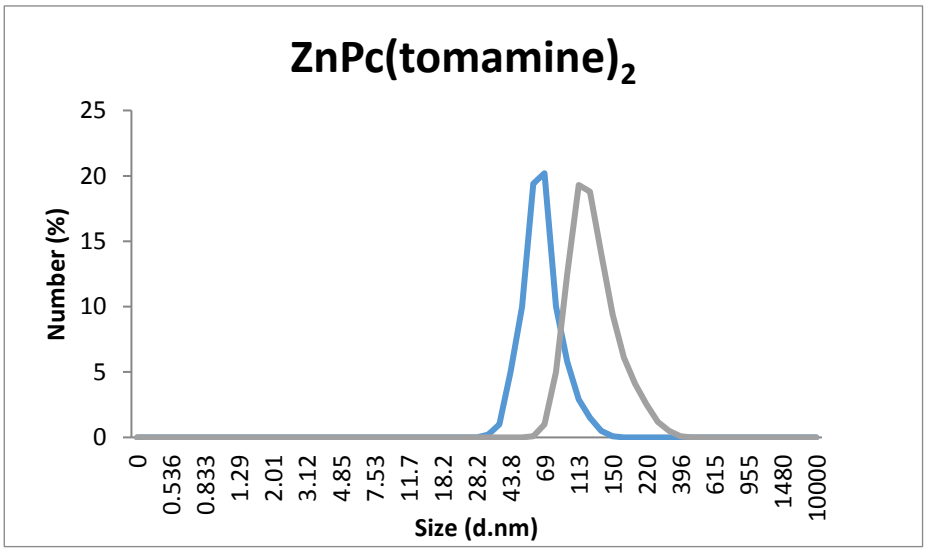

Figure S37. DLS of ZnPc(tomamine)$_2$ in acetone (blue) and PBS buffer (gray).

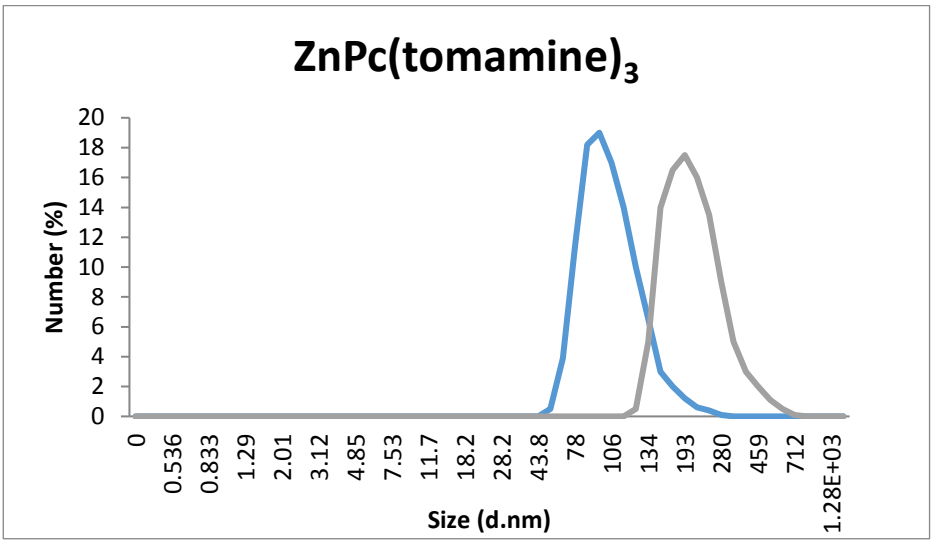

Figure S38. DLS of ZnPc(tomamine)$_3$ in acetone (blue) and PBS buffer (gray).

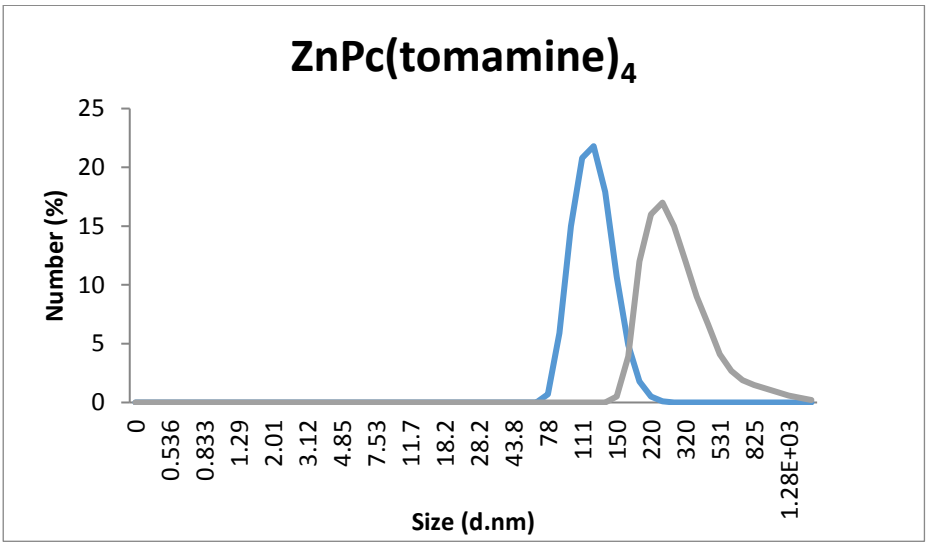

Figure S39. DLS of ZnPc(tomamine)$_4$ in acetone (blue) and PBS buffer (gray).

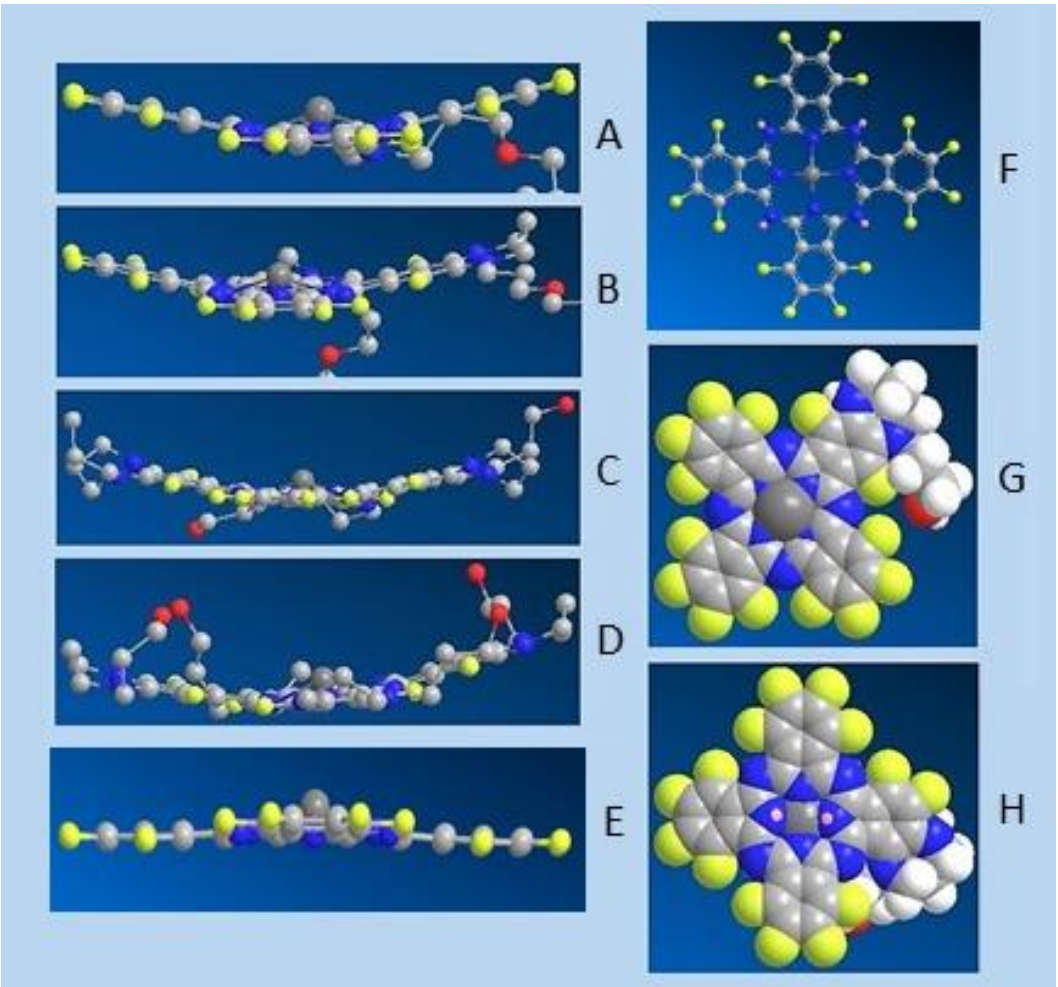

Figure S40. The side chains up to the oxygen and hydrogens are removed for clarity to highlight the distorted Pc of these MM2 steric energy minimized structures. (A) ZnPc(tomamine)$_1$, (B) ZnPc(tomamine)$_2$, (C) ZnPc(tomamine)$_3$, (D) ZnPc(tomamine)$_4$, (E) $ZnF_{16}Pc$ side-view, (F) $ZnF_{16}Pc$ top-view. Annealing these several times to 300 K and re-minimizing consistently results in the same distortions. (G) space filling model of ZnPc(tomamine)$_1$ appended to adjacent beta positions, (H) space filling model of ZnPc(tomamine)$_1$ where the primary amine is appended to a beta position and the secondary to the adjacent alpha position highlights the reason the latter is unreactive.

MM2 energy minimization.

The MM2 calculations were run on ChemOffice 3D with a minimum RMS gradient of 0.01, then molecular dymanics with a 2 fs interval were used to aneal the structure to 300 K, and the steric minimization was run again. This process was reapeated to assure that the minimimal geometry of the macrocycle was consistantly nonplanar. Similar procedures of the starting $ZnF_{16}Pc$ always yields a planar structure with the Zn(II) somewhat out of the plane of the isoindoles, consistent with crystal structures of similar complexes.

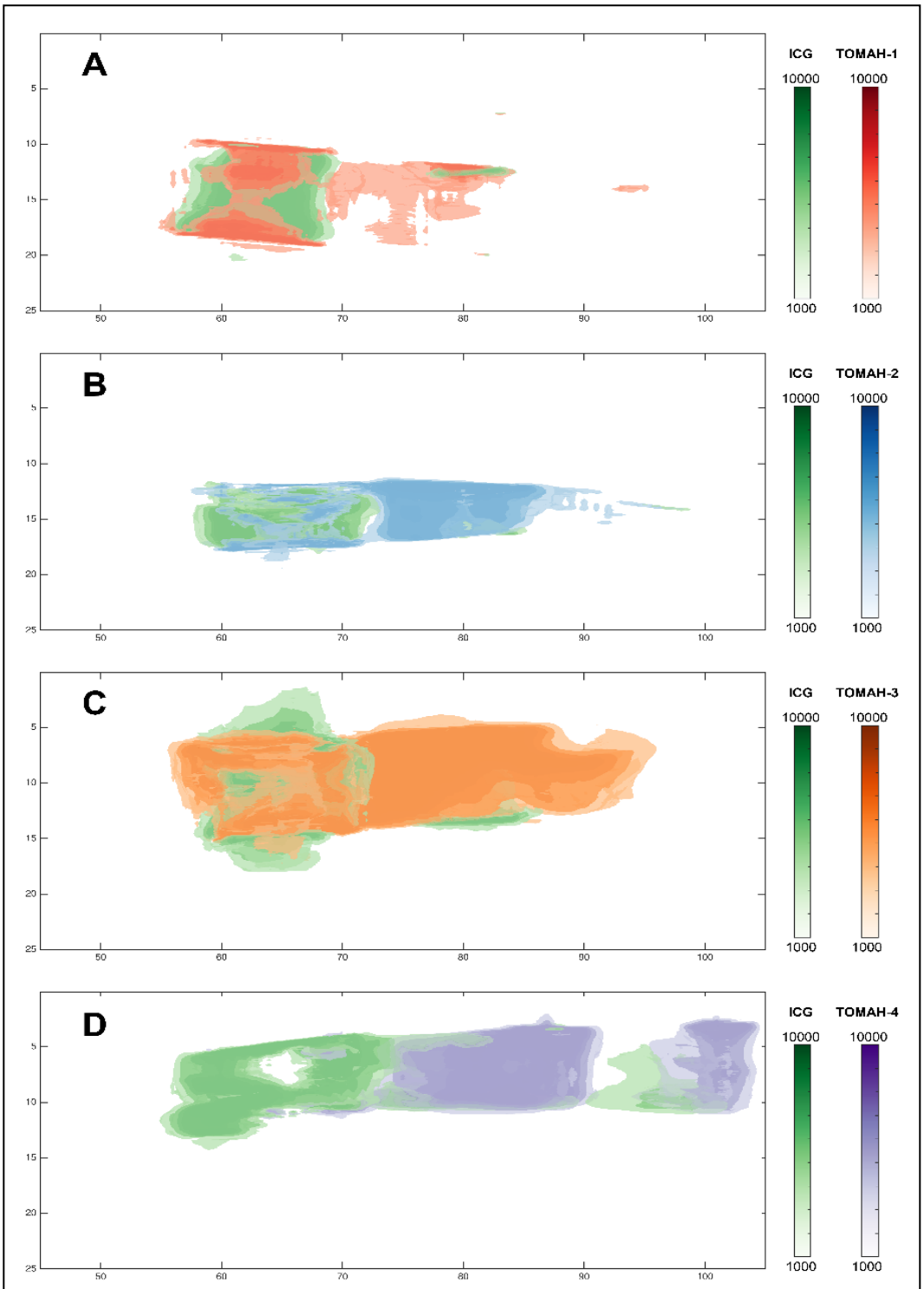

Figure S41. Photoacoustic 2-color images of (A) ZnPc(tomamine)$_1$, (B) ZnPc(tomamine)$_2$, (C) ZnPc(tomamine)$_3$, and (D) ZnPc(tomamine)$_4$ using a direct classical least-squares deconvolution technique.

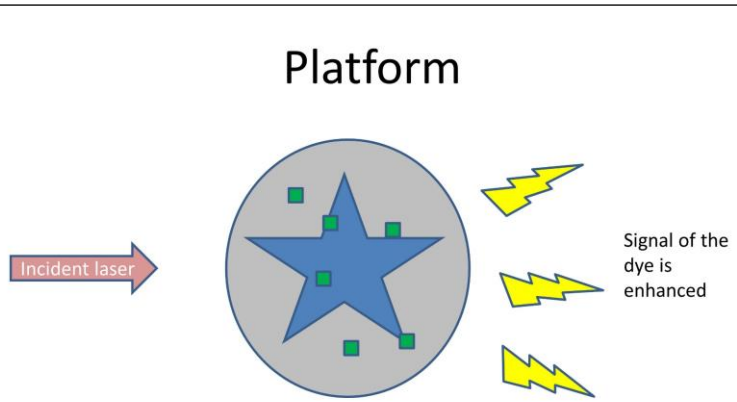

Figure S42. Dyes are adsorbed to the surface of gold stars through rapid silication. The electric field at the surface of gold enhances intrinsic Raman scattering. Targeting moieties can be conjugated to the silica to detect particular biomarkers at high sensitivity.

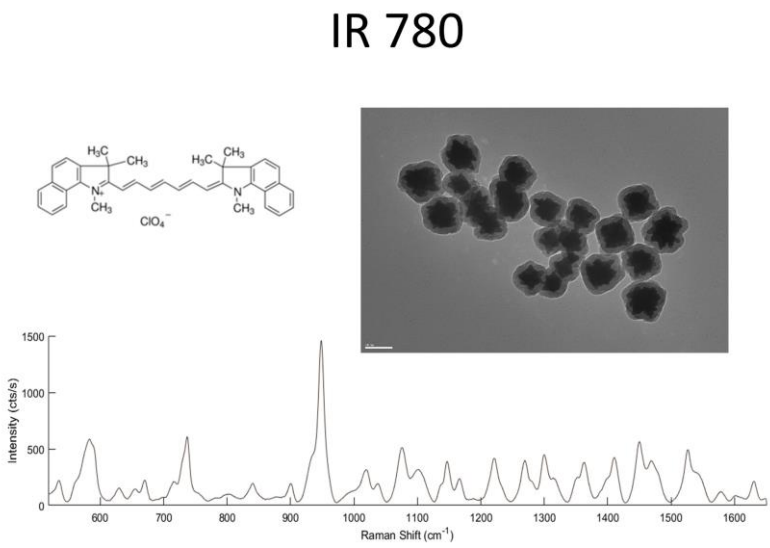

Figure S43. SERRS of IR 780 and TEM of the platform with this dye (scale bar = 100 nm).

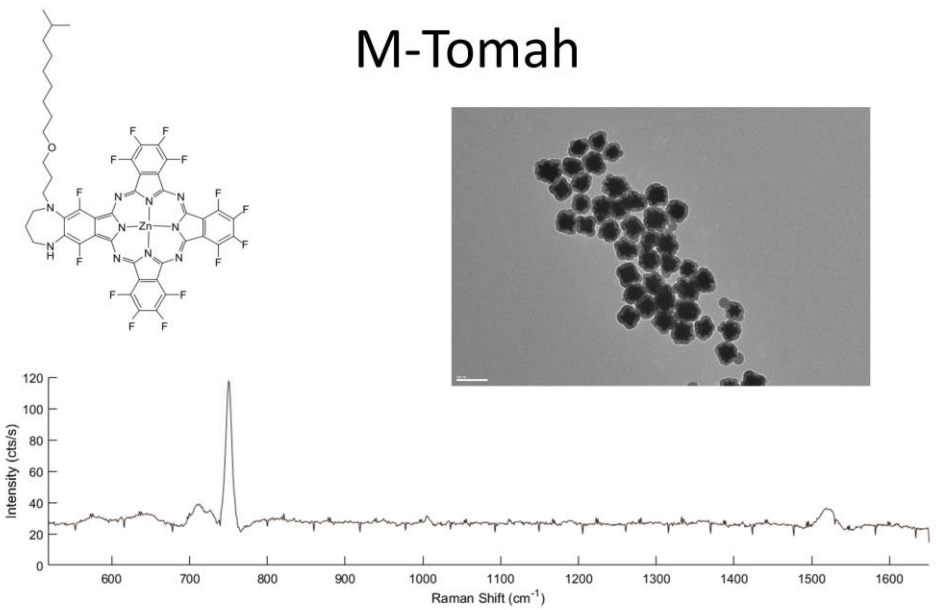

Figure S44. SERRS of the ZnPc(tomamine)$_1$ and TEM of the platform with this dye (scale bar = 200 nm).

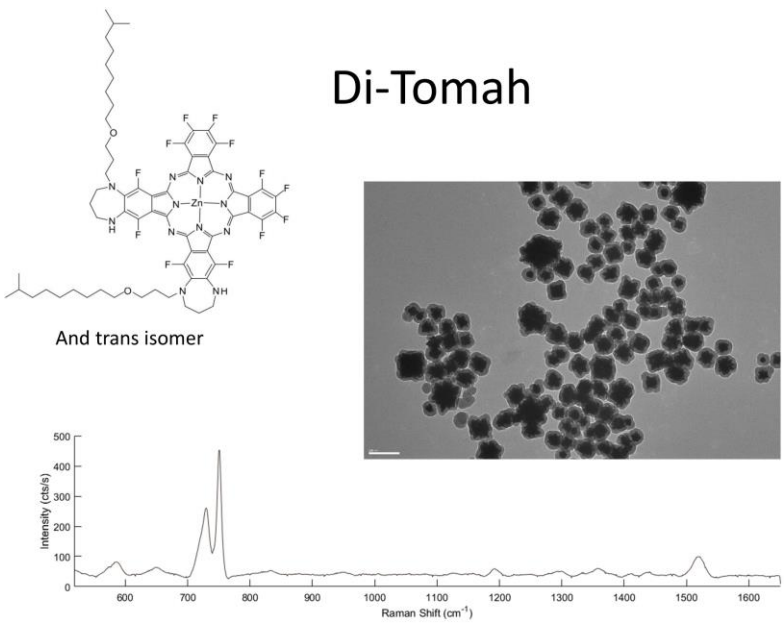

Figure S45. SERRS of the ZnPc(tomamine)$_2$ (mixture of cis and trans isomers) and TEM of the platform with this dye (scale bar = 200 nm).

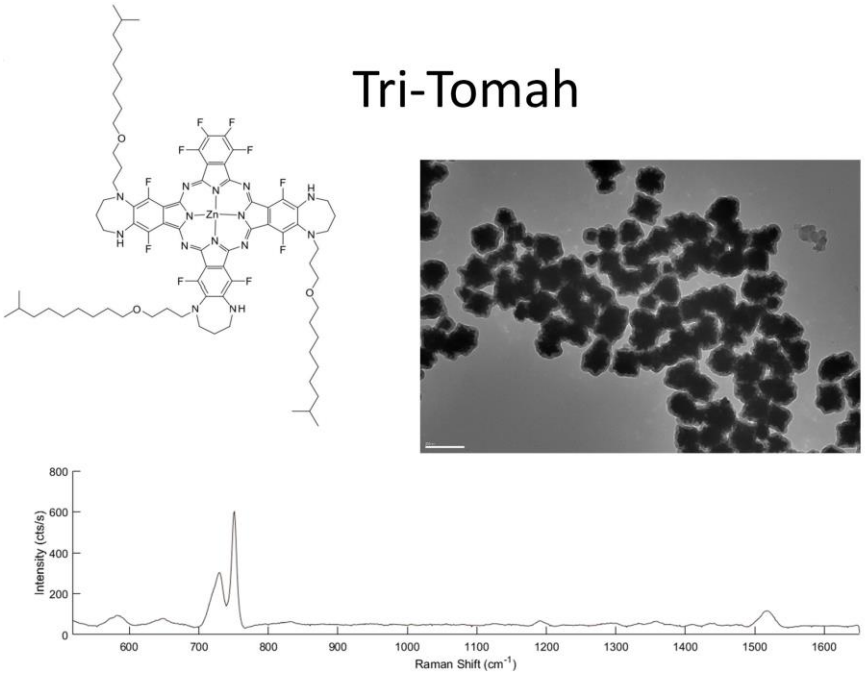

Figure S46. SERRS of the ZnPc(tomamine)$_3$ and TEM of the platform with this dye (scale bar = 200 nm).

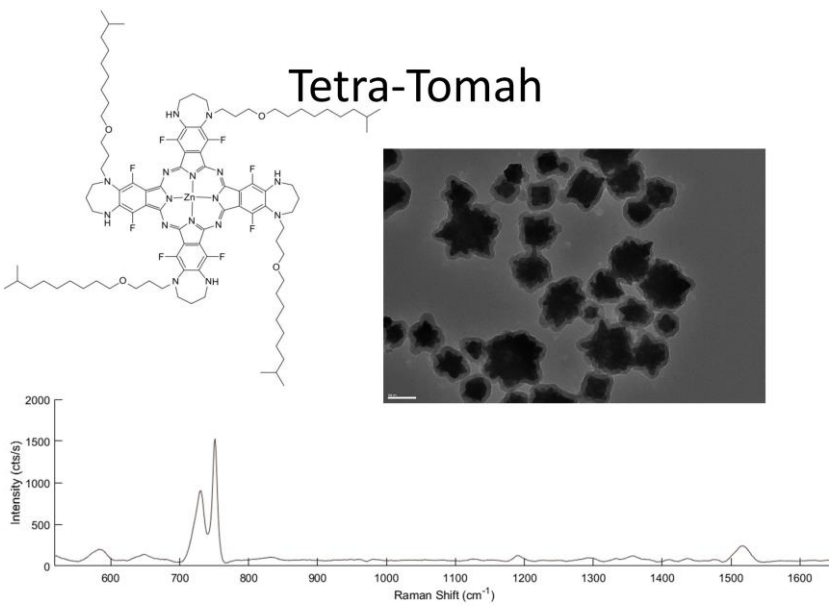

Figure S47. SERRS of the ZnPc(tomamine)$_4$ and TEM of the platform with this dye (scale bar = 200 nm).

ZnF16Pc

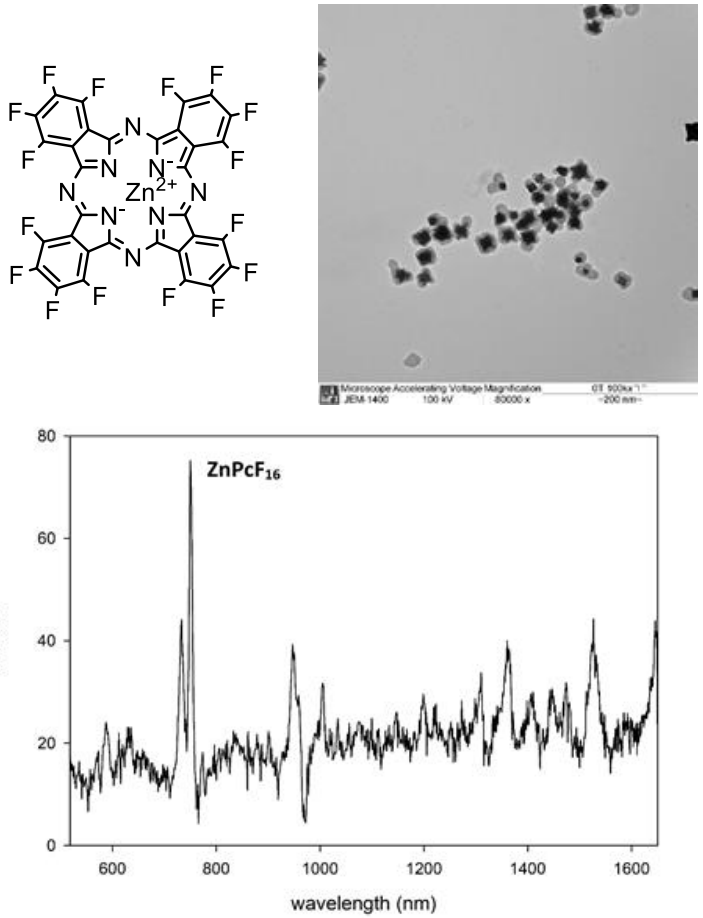

Figure S48. SERRS of the starting $ZnPcF_{16}$ platform on the gold nanostar nanoparticle and TEM of the platform with this dye (scale bar = 200 nm)

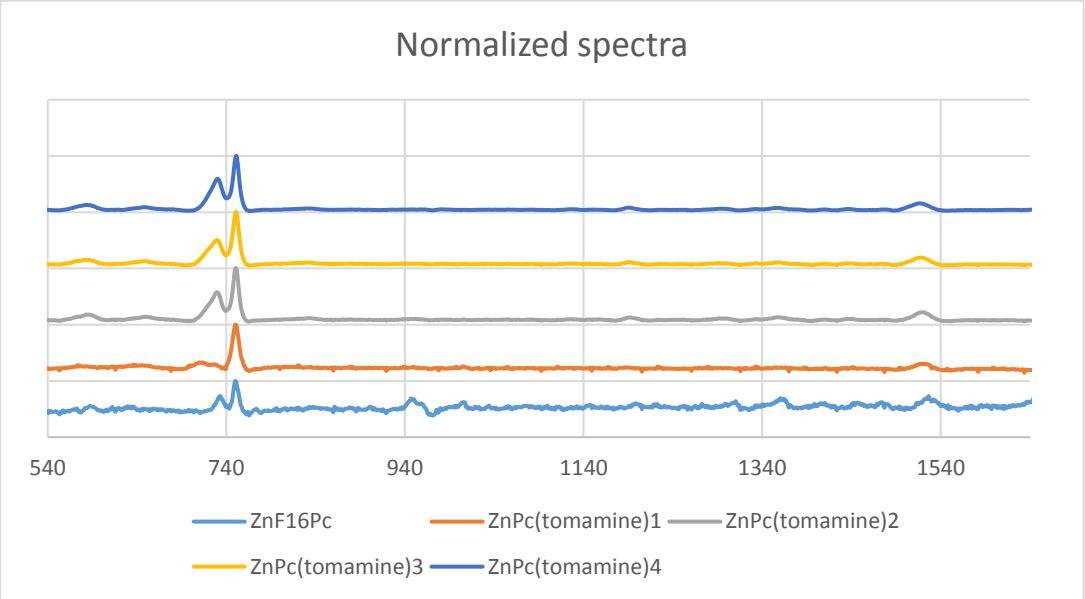

Figure S49. Normalized spectra of labeled particles

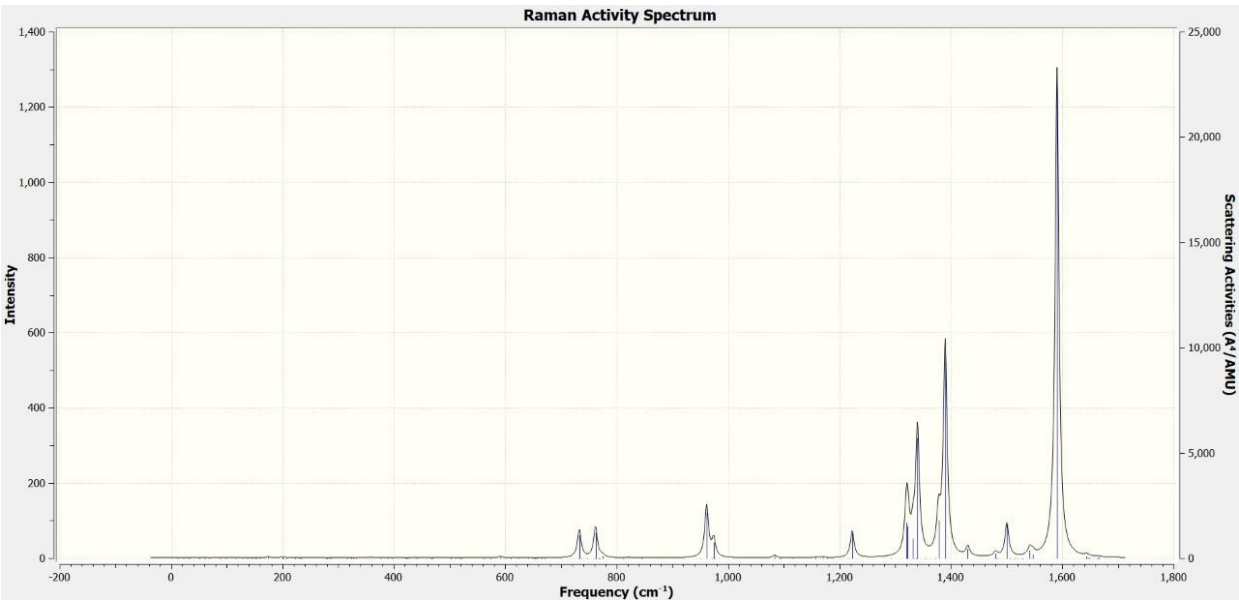

Figure S50. DFT calculated Raman spectra

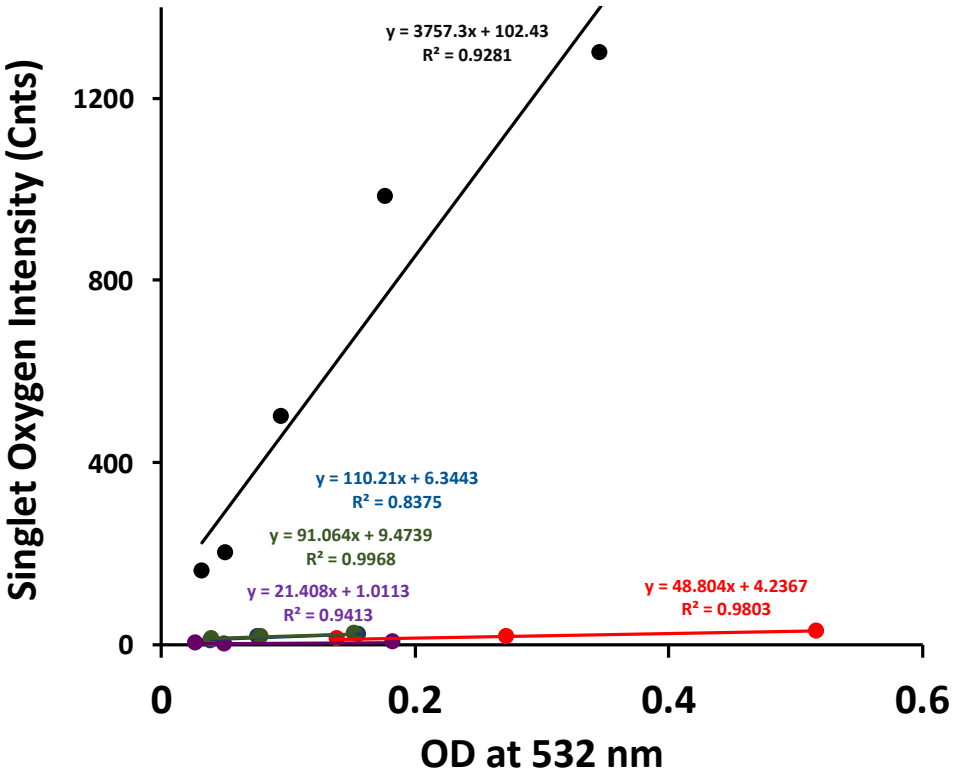

Figure S51. Measurements of singlet oxygen intensity at 1270 nm as a function of absorbance upon irradiation of rose bengal (black line), $(ZnPc(tomamine)_1$ (blue line), $ZnPc(tomamine)_2$ (red line), $ZnPc(tomamine)_3$ (green line) and $ZnPc(tomamine)_4$ (purple line) at 532 nm in d-acetone.

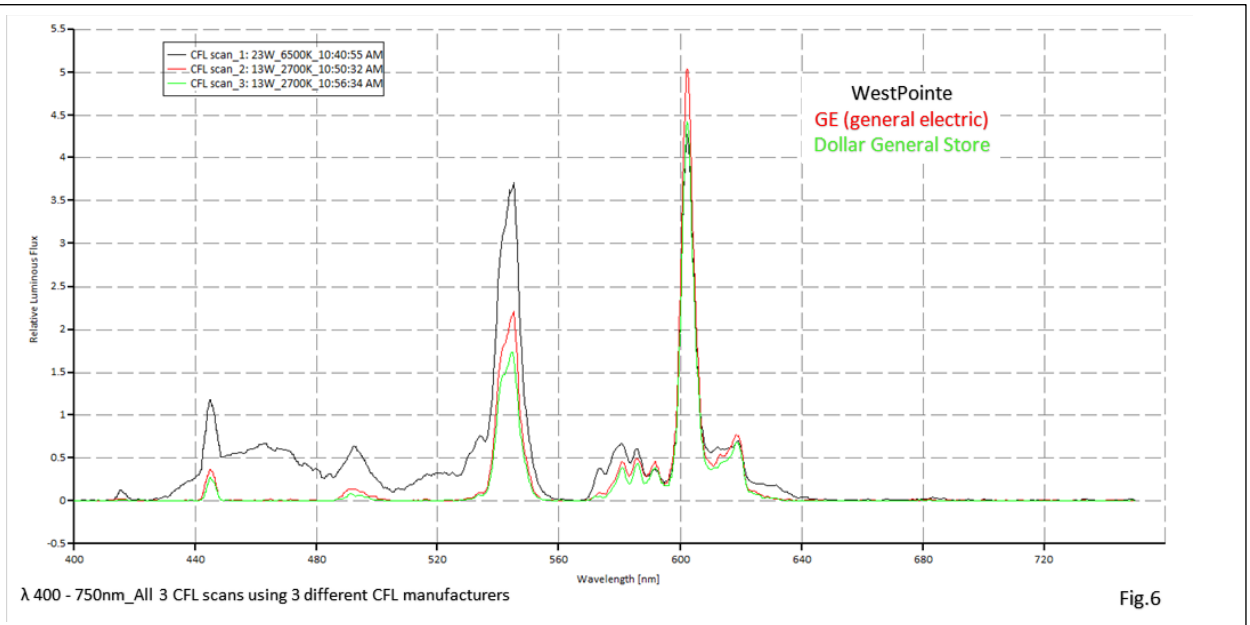

Figure S52. Spectrum of General Electric Helical 13W, 120V AC, 60 HZ, 190mA, (FLE13HT 2/2/XL.SW) fluorescent bulb taken from: https://publiclab.org/notes/dhaffnersr/09-06-2016/cfl-and-led-bulb-study-section-iii

Watts to lumens calculation

Energy saving lamps have high luminous efficacy (more lumens per watt).

The luminous flux Φ_V in lumens (lm) is equal to the power P in watts (W), times the luminous efficacy η in lumens per watt (lm/W):

$\Phi_{V(lm)} = P_{(W)} \times \eta_{(lm/W)}$

References

[1] I. M. Smallwood, *Handbook of Organic Solvent Properties*, Arnold, London, UK, **1996**.

[2] a) J.-P. Strachan, S. Gentemann, J. Seth, W. A. Kalsbeck, J. S. Lindsey, D. Holten, D. F. Bocian, *J. Am. Chem. Soc.* **1997**, *119*, 11191-11201; b) J. Chrysochoos, K. Beyene, *J. Luminesc.* **1999**, *81*, 209-218.

[3] T. S. Balaban, *Accounts of Chemical Research* **2005**, *38*, 612-623.

[4] J. P. Celli, B. Q. Spring, I. Rizvi, C. L. Evans, K. S. Samkoe, S. Verma, B. W. Pogue, T. Hasan, *Chemical Reviews* **2010**, *110*, 2795-2838.

[5] S. Singh, A. Aggarwal, N. V. S. D. K. Bhupathiraju, G. Arianna, K. Tiwari, C. M. Drain, *Chem. Rev.* **2015**, *115*, 10261-10306.

[6] S. Singh, A. Aggarwal, S. Thompson, J. P. C. Tomé, X. Zhu, D. Samaroo, M. Vinodu, R. Gao, C. M. Drain, *Bioconj. Chem.* **2010**, *21*, 2136-2146.

[7] V. Neuschmelting, N. C. Burton, H. Lockau, A. Urich, S. Harmsen, V. Ntziachristos, M. F. Kircher, *Photoacoustics* **2016**, *4*, 1-10.

[8] V. Neuschmelting, H. Lockau, V. Ntziachristos, J. Grimm, M. F. Kircher, *Radiology* **2016**, *280*, 137-150.

[9] P. Beard, *Interface Focus* **2011**, *1*, 602-631.

[10] X. M. Qian, S. M. Nie, *Chem. Soc. Rev.* **2008**, *37*, 912-920.

[11] a) M. Fleischmann, P. J. Hendra, A. J. McQuillan, *Chem. Phys. Let.* **1974**, *26*, 163-166; b) J. F. Li, Y. F. Huang, Y. Ding, Z. L. Yang, S. B. Li, X. S. Zhou, F. R. Fan, W. Zhang, Z. Y. Zhou, D. Y. Wu, B. Ren, Z. L. Wang, Z. Q. Tian, *Nature* **2010**, *464*, 392.

[12] a) G. McNay, D. Eustace, W. E. Smith, K. Faulds, D. Graham, *Appl. Spectrosc.* **2011**, *65*, 825-837; b) B. Sharma, R. R. Frontiera, A.-I. Henry, E. Ringe, R. P. Van Duyne, *Mater. Today* **2012**, *15*, 16-25.

[13] M. A. Wall, S. Harmsen, S. Pal, L. Zhang, G. Arianna, J. R. Lombardi, C. M. Drain, M. F. Kircher, *Adv. Mater.* **2017**, *29*, 1605622.

[14] a) Z.-Q. Tian, B. Ren, D.-Y. Wu, *J. Phys. Chem. B* **2002**, *106*, 9463-9483; b) S. L. Kleinman, R. R. Frontiera, A.-I. Henry, J. A. Dieringer, R. P. Van Duyne, *Phys. Chem. Chem. Phys.* **2013**, *15*, 21-36.

[15] E. C. Le Ru, E. Blackie, M. Meyer, P. G. Etchegoin, *J. Phys. Chem. C* **2007**, *111*, 13794-13803.

[16] W. E. Doering, S. Nie, *Anal. Chem.* **2003**, *75*, 6171-6176.

[17] C. C. Leznoff, J. L. Sosa-Sanchez, *Chemical Communications* **2004**, 338-339.

[18] R. V. Belosludov, D. Nevonen, H. M. Rhoda, J. R. Sabin, V. N. Nemykin, *The Journal of Physical Chemistry A* **2019**, *123*, 132-152.

[19] a) A. Aggarwal, S. Singh, Y. Zhang, M. Anthes, D. Samaroo, R. Gao, C. M. Drain, *Tetrahedron Letters* **2011**, *52*, 5456-5459; b) S. Silva, P. M. R. Pereira, P. Silva, F. A. Almeida Paz, M. A. F. Faustino, J. A. S. Cavaleiro, J. P. C. Tomé, *Chemical Communications* **2012**, *48*, 3608-3610.

[20] C. Farley, N. V. S. D. K. Bhupathiraju, B. K. John, C. M. Drain, *J. Phys. Chem. A* **2016**, *120*, 7451-7464.

[21] a) T. Honda, T. Kojima, N. Kobayashi, S. Fukuzumi, *Angew. Chem. Int. Ed.* **2011**, *50*, 2725-2728; b) S. M. Yoon, H. J. Song, I.-C. Hwang, K. S. Kim, H. C. Choi, *Chem. Com.* **2010**, *46*, 231-233.

[22] C. Farley, A. Aggarwal, S. Singh, A. Dolor, P. To, A. Falber, M. Crossley, C. M. Drain, *Journal of Computational Chemistry* **2018**, *39*, 1129-1142.

[23] a) H. Jiang, J. Ye, P. Hu, F. Wei, K. Du, N. Wang, T. Ba, S. Feng, C. Kloc, *Scientific Reports* **2014**, *4*, 7573; b) L.-Y. Cui, J. Yang, Q. Fu, B.-Z. Zhao, L. Tian, H.-L. Yu, *J. Mol. Structure* **2007**, *827*, 149-154.

[24] a) V. Kavelin, O. Fesenko, H. Dubyna, C. Vidal, T. A. Klar, C. Hrelescu, L. Dolgov, *Nanoscale Res. Let.* **2017**, *12*, 197; b) D. R. Tackley, G. Dent, W. Ewen Smith, *Phys. Chem. Chem. Phys.* **2001**, *3*, 1419-1426; c) D. R. Tackley, G. Dent, W. Ewen Smith, *Physical Chemistry Chemical Physics* **2000**, *2*, 3949-3955.

[25] E. E. Ferguson, R. L. Hudson, J. R. Nielsen, D. C. Smith, *J. Chem. Phys.* **1953**, *21*, 1464-1469.

[26] T. J. Russin, E. İ. Altinoğlu, J. H. Adair, P. C. Eklund, *Journal of Physics: Condensed Matter* **2010**, *22*, 334217.

[27] S. Mathai, T. A. Smith, K. P. Ghiggino, *Photochem. Photobio. Sci.* **2007**, *6*, 995-1002.

[28] W. Li, W. Lu, Z. Fan, X. Zhu, A. Reed, B. Newton, Y. Zhang, S. Courtney, P. T. Tiyyagura, R. R. Ratcliff, S. Li, E. Butler, H. Yu, P. C. Ray, R. Gao, *J. Mat. Chem.* **2012**, *22*, 12701-12708.